

**Role of Ste-20 Like Kinase, SLK, in Focal Adhesion
Complexes in Podocytes**

Craig Bryan
Department of Experimental Medicine
McGill University, Montreal

Supervisor: Dr. Andrey Cybulsky
Date of submission: July 27, 2022

A thesis submitted to McGill University in partial fulfilment of the requirements of the degree
of Master of Science in Experimental Medicine

© Craig Bryan, 2022

Table of Contents

<i>Abstract</i>	5
<i>Résumé</i>	8
<i>Acknowledgments</i>	11
<i>Contributions of Authors</i>	12
<i>List of Abbreviations</i>	13
<i>List of Figures</i>	14
Chapter 1: Introduction	16
1.1 Kidney and podocyte structure	16
1.1.1 Glomerular structure	16
1.1.2 Podocyte and foot processes	18
1.2 Podocyte cytoskeleton	21
1.2.1 Actin cytoskeleton	21
1.2.2 Focal adhesion complexes	23
1.2.3 Integrin	23
1.2.4 Focal adhesion proteins.....	24
1.3 SLK	28
1.3.1 SLK structure	29
1.3.2 SLK activation and function	29
1.3.3 SLK Activity in the kidney and in podocytes	29
1.3.4 SLK effect on focal adhesion complexes.....	30

<i>Chapter 2: Rationale and Hypothesis</i>	32
Rationale	32
Hypothesis	33
<i>Chapter 3: Materials and Methods</i>	34
3.1 Antibodies and reagents:	34
3.2 Generation of SLK knockout (KO) glomerular epithelial cell clones:	35
3.3 Cell Culture:	35
3.4 Measurement of Adriamycin cytotoxicity:	36
3.5 Generation and treatment of SLK KO mice:	37
3.6 Immunofluorescence (IF) microscopy	37
3.7 Kidney sections	38
3.8 Image Analysis	39
3.9 Western blotting/Immunoblotting	40
3.10 Statistics	41
<i>Chapter 4: Results</i>	42
4.1 SLK deletion increases small vinculin, paxillin and talin particles number and decreases large paxillin particle number.	42
4.2 SLK deletion increases adhesion area of small vinculin particles and large talin particles.	48
4.3 SLK deletion does not alter vinculin, paxillin, and talin particle size.	51

4.4 SLK deletion decreases particle number and adhesion area in glomerular epithelial cells treated with Adriamycin.	51
4.5 SLK deletion does not alter paxillin and vinculin colocalization.	53
4.5 SLK deletion does not alter total expression of focal adhesion proteins.	55
4.6 SLK deletion increases talin and nephrin colocalization in mouse glomeruli.	58
<i>Chapter 5: Discussion</i>.....	64
5.1 Conclusion	68
5.2 Future Directions	69
5.2.1 Colocalization experiments between talin and β 1 integrin or α 5 collagen.....	69
5.2.2 Investigating the SLK phosphorylation of paxillin and mammalian talin in GECs	
70	
<i>Chapter 6: References</i>	71

Abstract

Glomerular diseases are characterized by a disruption of glomerular permselectivity, often due to damage to glomerular epithelial cells (GECs) or podocytes, which are highly differentiated cells in the glomerular capillary wall. Mechanisms underlying podocyte damage converge on disruption of the cytoskeleton. The Ste20-like kinase SLK is a serine/threonine protein kinase which regulates organ development, cell migration, cytokinesis, and cytoskeletal structure. While global deletion of SLK in mice is lethal during embryogenesis, mice with podocyte-specific deletion of SLK show increased glomerular filtration barrier dysfunction and podocyte injury. SLK phosphorylates and activates ezrin, which localizes ezrin to the apical membrane of the podocyte foot processes. The phosphorylated ezrin forms a complex with podocalyxin and the Na⁺/H⁺ exchanger regulatory factor (NHERF2), which connects to F-actin to maintain cellular polarity and podocyte structure. Previous studies have shown that SLK phosphorylates paxillin (a multi-domain focal adhesion adapter protein) in fibroblasts, resulting in regulation of focal adhesion turnover and cell migration. In *Drosophila*, the SLK homolog SLIK phosphorylates talin-1, a component of focal adhesions; and this phosphorylation is crucial for muscle attachment. The present study aims to identify substrates of SLK, by which SLK regulates cytoskeletal structure in podocytes. This study focuses on focal adhesion components paxillin, vinculin and talin.

Primary cultured GECs were established from mice with a floxed SLK allele. Cells were transduced with Cre recombinase to delete SLK. Adriamycin is a nephrotoxin that induces glomerular injury *in vivo*, in part by inducing actin depolymerization thereby disrupting

cytoskeletal structure in GECs. Expression and localization of paxillin, vinculin and talin in focal adhesion complexes in SLK knockout (KO) and control GECs (with and without Adriamycin treatment) were evaluated using immunofluorescence microscopy. Kidney sections derived from treated and untreated SLK KO and control mice were examined for talin and nephrin expression and colocalization via immunofluorescence microscopy.

We examined small and large particles of vinculin, paxillin and talin to determine whether SLK regulates the size, number, and area of focal adhesion complexes. Deletion of SLK in GECs results in an increase in small vinculin, paxillin, and talin particles along with increases in the adhesion area of small vinculin particles and large talin particles. This suggests that SLK deletion may reduce phosphorylation of paxillin particles, resulting in greater retention of vinculin and talin particles in focal adhesions. In GECs treated with Adriamycin, SLK deletion decreases particle number and adhesion area, suggesting that SLK KO GECs may be more susceptible to cell injury than treated control GECs.

In vivo, deletion of SLK in podocytes results in focal effacement of foot processes. To address the effect of SLK on the localization of focal adhesion complexes *in vivo*, we examined the colocalization of talin with nephrin in mouse glomeruli. Nephrin (a component of the podocyte slit diaphragm) is situated basolaterally in podocytes; thus, we hypothesized that increased colocalization of talin with nephrin would reflect an increase in podocyte focal adhesions. Indeed, SLK deletion increases the colocalization of talin and nephrin. Thus, SLK deletion may impair the turnover to formation ratio of talin particles and result in an abundance of talin particles in the basolateral aspect of podocytes. This initial increase in podocyte focal adhesions during foot process effacement results in increased adhesion to the

glomerular basement membrane to prevent podocyte loss. Treated SLK KO mice were more susceptible to Adriamycin treatment and were unable to mount the same adaptive response as treated control mice resulting in an overall decrease in colocalization of talin and nephrin.

In summary, these results suggest that SLK regulates the composition of focal adhesion complexes, which can then affect adhesion of podocytes to the glomerular basement membrane.

Résumé

Les maladies glomérulaires sont caractérisées par une perturbation de la perméabilité glomérulaire, souvent due à des lésions aux cellules épithéliales glomérulaires (GEC) ou des podocytes, qui sont des cellules hautement différenciées de la paroi capillaire glomérulaire. Les mécanismes sous-jacents aux lésions des podocytes convergent vers une perturbation du cytosquelette. La kinase de type Ste20 SLK est une protéine kinase de type sérine/thréonine qui régule le développement des organes, la migration cellulaire, la cytokinèse et la structure du cytosquelette. Bien qu'une délétion complète de SLK soit létale pendant l'embryogenèse chez la souris, les souris avec une délétion de SLK étant spécifique aux podocytes présentent un dysfonctionnement accru de la barrière de filtration glomérulaire et des lésions podocytaires. SLK phosphoryle et active l'eitrine, ce qui a pour effet de localiser l'eitrine à la membrane apicale des pédicelles podocytaires. L'eitrine phosphorylée forme un complexe avec la podocalyxine et le facteur de régulation de l'échangeur Na⁺/H⁺ (NHERF2), qui se connecte à la F-actine pour maintenir la polarité cellulaire et la structure des podocytes. Des études antérieures ont montré que SLK phosphoryle la paxilline (une protéine adaptatrice d'adhérence focale à multiples domaines) dans les fibroblastes, ce qui entraîne la régulation du renouvellement des adhérences focales et de la migration cellulaire. Chez la drosophile, l'homologue de SLK, SLIK, phosphoryle la taline-1, un composant des adhérences focales : cette phosphorylation étant cruciale pour l'attachement musculaire. Cette étude vise à identifier les substrats de SLK, par lesquels SLK régule la structure cytosquelettique dans les podocytes. Cette étude se concentre sur les composants des adhérence focales : la paxilline, la vinculine et la taline.

Des cultures primaires de GEC ont été établies à partir de souris avec un allèle SLK floxé. Les cellules ont été transduites avec la recombinaison Cre pour supprimer SLK. L'adriamycine est une néphrotoxine qui induit des lésions glomérulaires *in vivo*, en partie en induisant une dépolymérisation de l'actine, perturbant ainsi la structure du cytosquelette dans les GEC. L'expression et la localisation de la paxilline, de la vinculine et de la taline dans les complexes d'adhérences focales des GECs de contrôle et SLK knockout (KO) (avec et sans traitement à l'Adriamycine) ont été évaluées par microscopie à immunofluorescence. Des coupes de rein dérivées de souris SLK KO et de contrôle traitées et non traitées ont été examinées pour l'expression et la colocalisation de la taline et de la néphrine par microscopie à immunofluorescence.

Nous avons examiné les petites et grandes particules de vinculine, de paxilline et de taline pour déterminer si SLK régule la taille, le nombre et la surface des complexes d'adhérences focales. Une délétion de SLK dans les GECs entraîne une augmentation des petites particules de vinculine, de paxilline et de taline ainsi qu'une augmentation de la zone d'adhésion des petites particules de vinculine et des grandes particules de taline. Cela suggère qu'une délétion de SLK peut réduire la phosphorylation des particules de paxilline, ce qui entraîne une plus grande rétention des particules de vinculine et de taline dans les adhérences focales. Dans les GECs traités à l'Adriamycine, une délétion de SLK diminue le nombre de particules ainsi que la zone d'adhérence, ce qui suggère que les GECs SLK KO pourraient être plus sensibles aux lésions cellulaires que les GECs de contrôle traitées.

In vivo, une délétion de SLK dans les podocytes entraîne un effacement focal des pédicelles. Pour étudier l'effet de SLK sur la localisation des complexes d'adhérences focales *in vivo*,

nous avons examiné la colocalisation de la taline avec la néphrine dans les glomérules de souris. La néphrine (un composant du diaphragme de fente des podocytes) est située à la base des podocytes : nous avons donc émis l'hypothèse qu'une colocalisation accrue de la taline avec la néphrine refléterait une augmentation des adhérence focales des podocytes. En effet, une délétion de SLK augmente la colocalisation de la taline et de la néphrine. Ainsi, une délétion de SLK peut altérer le rapport entre le renouvellement et la formation des particules de taline et entraîner une abondance de particules de taline dans l'aspect basolatéral des podocytes. Cette augmentation initiale des adhérences focales des podocytes pendant l'effacement des pédicelles entraîne une augmentation de l'adhérence à la membrane basale glomérulaire pour prévenir la perte des podocytes. Les souris SLK KO traitées ont été plus sensibles au traitement par Adriamycine et n'ont pas été en mesure d'organiser la même réponse adaptative que les souris de contrôle traitées, ce qui a entraîné une diminution globale de la colocalisation de la taline et de la néphrine.

En résumé, ces résultats suggèrent que SLK régule la composition des complexes d'adhésion focaux, ce qui peut ensuite affecter l'adhésion des podocytes à la membrane basale glomérulaire.

Acknowledgments

I would like to express my sincere gratitude to my supervisor, Dr. Andrey Cybulsky, for welcoming me into his lab and for his patience and guidance during my graduate studies. I would also like to thank the members of my thesis committee: Dr. Nathalie Lamarche-Vane, Dr. Elena Torban, and Dr. Danuta Radzioch, for their critical input and guidance on my project. Special thanks to my lab colleagues Julie Guillemette and Joan Papillon who taught me the lab techniques I used in my experiments. I would like to extend my thanks to everyone in the Nephrology division, especially Lamine Aoudjit, Sajida Ibrahim, and Sima Babaveya, who readily provided technical support and suggestions for my protocols. I would like to express my appreciation to Dr. Aimee Ryan and her lab as well as Dr. Loydie Majewska for their academic and professional guidance during my time at the Research Institute of the McGill University Health Centre. I would not be able to write this thesis without the support of Dr. Sheri McDowell (and her numerous revisions) and Fio Vialard (for their revisions and French translation). Special thanks to Dina Greenberg for teaching me how to use the GraphPad software and her revisions of my thesis drafts. I am thankful for the scholarship I received from the Black Business and Professional Association in 2020.

Lastly, I would like to thank my core support group: my parents (Margaret and Relva), my mother-in-law (Velma) and my partner, Natoya, who all provided me with unwavering support from the beginning till the end.

I dedicate this thesis to my grandfather, Orrett Plummer, who died from complications of ESRD.

Contributions of Authors

Julie Guillemette and Joan Papillon cut and cryopreserved the tissue sections from the SLK KO mice that were used in the Talin/Nephrin double staining experiments. Boyan Woychyshyn and Joan Papillon generated and immortalized the SLK KO glomerular epithelial cells used in most of the experiments.

All other experimental work was done by Craig Bryan.

List of Abbreviations

ADR- Adriamycin

BSA- Bovine Serum Albumin

CTRL- Control

ESRD- End Stage Kidney Disease

FP- Foot Process

FSGS- Focal Segmental Glomerulosclerosis

IF- Immunofluorescence Microscopy

IgG- Immunoglobulin G

GEC- Glomerular Epithelial Cells (Podocytes)

KO- Knockout

MOC1- Manders Overlap Coefficient 1

MOC2- Manders Overlap Coefficient 2

PCC- Pearson Correlation Coefficient

PBS- Phosphate Buffered Saline

PFA- Paraformaldehyde

SD- Slit Diaphragm

SEM- Standard Error of the Mean

SLK- Ste20-like Kinase

SV40- Simian Virus 40

WB- Western Blot

WT1- Wilms Tumor 1

List of Figures

Figure 1: Podocytes are terminally differentiated cells within the glomerulus.	17
Figure 2: Schematic showing the slit diaphragm, focal adhesions, and actin regulatory proteins in podocytes.	20
Figure 3: Focal adhesions provide both a structural and signaling link between the extracellular matrix and the actin cytoskeleton.	22
Figure 4: Structure of SLK molecule (1204 amino acids) showing the kinase domain, phosphorylation sites and coiled-coil (CC) domain.....	28
Figure 5: Representative images of immunofluorescence staining of focal adhesion proteins in Control (Ctrl) and SLK Knockout (KO) GECs.	44
Figure 6: SLK deletion increases small vinculin, paxillin and talin particle numbers and decreases paxillin large particle number.	46
Figure 7: SLK deletion increase adhesion area of small vinculin particles and large talin particles.	49
Figure 8: SLK deletion does not substantially alter small and large paxillin, vinculin and talin particle sizes.....	52
Figure 9: Effect of SLK deletion on paxillin-vinculin colocalization.	54
Figure 10: Immunoblot showing Control and SLK KO GECs at 33°C (proliferation), 37°C (differentiation) and with Adriamycin treatment.	56
Figure 11: Representative images of talin (red) and nephrin (green) staining in (A) untreated and (B) Adriamycin treated (ADR Tx) control and SLK KO mice glomeruli sections.	59
Figure 12: Deletion of SLK increases talin-nephrin colocalization.....	61

Figure 13: Deletion of SLK does not alter (A) talin and nephrin immunofluorescence intensity or (B) glomerular total area.....63

Chapter 1: Introduction

1.1 Kidney and podocyte structure

1.1.1 Glomerular structure

The glomerulus is a highly specialised structure that functions as the filtration unit of the kidney, and at the same time prevents the leakage of proteins into the glomerular filtrate. It is composed of mesangial cells, glomerular endothelial cells, and glomerular epithelial cells, all encapsulated by the glomerular parietal epithelial cells (which make up the Bowman's capsule) (**Figure 1**) [1, 2]. The glomerular endothelial and epithelial cells, along with the glomerular basement membrane (GBM) form the glomerular capillary wall. Defects in the glomerular capillary wall at any at any level can result in loss of essential proteins in the urine (proteinuria).

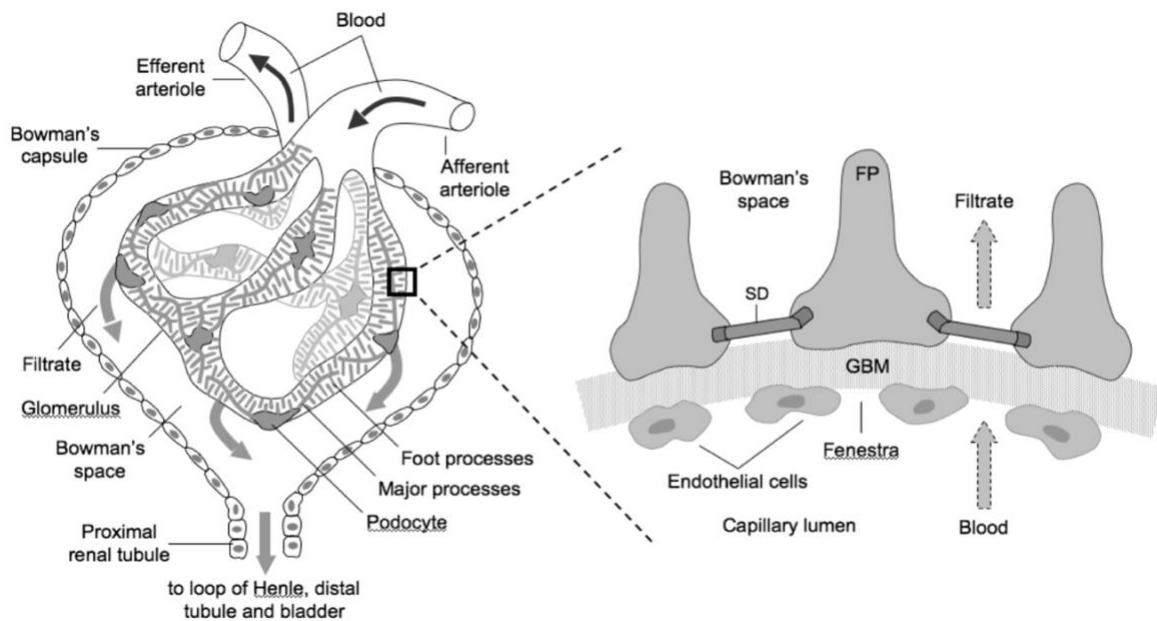


Figure 1: Podocytes are terminally differentiated cells within the glomerulus. Their most prominent features are interdigitated foot processes (FP) that rest on the glomerular basement membrane (GBM) and are interconnected by slit diaphragms (SD). This figure is adapted from [Reiser, J., M. Altintas, K. Ulgen, D. Palmer-Toy, V. Shih, and D. Kompala, Emerging Roles for Metabolic Engineering - Understanding Primitive and Complex Metabolic Models and Their Relevance to Healthy and Diseased Kidney Podocytes. Current Chemical Biology, 2008. 2: p. 68-82., License ID: 1252007-2] [3]

1.1.2 Podocyte and foot processes

Glomerular epithelial cells (GECs), also known as podocytes, are a key component of the glomerular filtration barrier. Podocytes are highly specialized, terminally differentiated cells, with cell bodies that extend primary processes that further branch into secondary and tertiary major processes (**Figure 1**) [4-7]. These secondary and tertiary major processes divide into long, interdigitating structures (foot processes) which cover the surface of the capillary loops, and thereby uphold the integrity of the glomerular filtration barrier [1, 8]. These foot processes adhere to the extracellular surface of the glomerular basement membrane and are joined laterally by slit diaphragms.

Glomerular disease is characterized by glomerular filtration barrier dysfunction, in part, due to damage of GECs, resulting in flattening and effacement of podocyte foot processes [4, 6]. A host of diseases can disrupt the filtration barrier, including genetic and acquired diseases [9]. Focal segmental glomerulosclerosis (FSGS) is a glomerulopathy that may present as nephrotic syndrome and is characterized by sclerosis, hyalinosis and adhesion formation resulting in the segmental scarring of some (focal) glomeruli [10, 11]. FSGS may be categorized as primary (idiopathic) or secondary (which may be due to genetic, drug-induced or viral associated factors [11].) Adaptive structural or functional responses to several stimuli due to glomerular hypertrophy and hyperfiltration can also result in secondary FSGS [12].

The podocyte slit diaphragm is a size selective barrier between two podocyte foot processes that prevents filtration of large macromolecules into the ultrafiltrate. Slit diaphragms contain proteins expressed in adherens and tight junctions as well as proteins unique to podocytes such as nephrin and podocin [4, 13]. Nephrin is a 180 kDa protein and an important

component of the slit diaphragm [14]. Previous studies have shown that nephrin phosphorylation signalling can regulate actin polymerisation in the podocyte [15]. Nephrin can also bind to the adaptor protein CD2-associated protein (CD2AP) which interacts directly with actin and synaptopodin thus serving as a direct link of the slit diaphragm and the actin cytoskeleton [15]. Mice with podocyte-specific deletion of nephrin (*Nphs1* deletion) had foot process structural abnormalities and massive proteinuria at 1-week of age [16, 17]. Furthermore, intravenous administration of a monoclonal anti-nephrin antibody in mice established a murine FSGS model thereby highlighting the importance of the nephrin in preventing proteinuria [18, 19].

Podocytes remodel their shape when they are exposed to significant stress by external forces [20, 21]. During foot process effacement, the slit diaphragms disappear or are displaced from their usual position at the base of the foot process, and there is retraction of the foot processes into the cell body resulting in increased adherence to the GBM [20, 22]. This process is thought to reflect a derangement of the actin cytoskeleton which leads to structural and functional changes. Thus, an intricate framework supported by the actin skeletal structure, including filtration slit diaphragms and focal adhesion complexes, is important for adhesion to the glomerular basement membrane and the maintenance of the filtration barrier [23, 24].

Foot process effacement is thought to be a survival strategy to increase cell attachment to the GBM thereby preventing cell detachment from the GBM and prevent podocyte loss. [22, 25, 26]. Persistent or more severe injury can lead to cell detachment and subsequent podocyte loss in the urinary space resulting in further glomerular damage [22, 26].

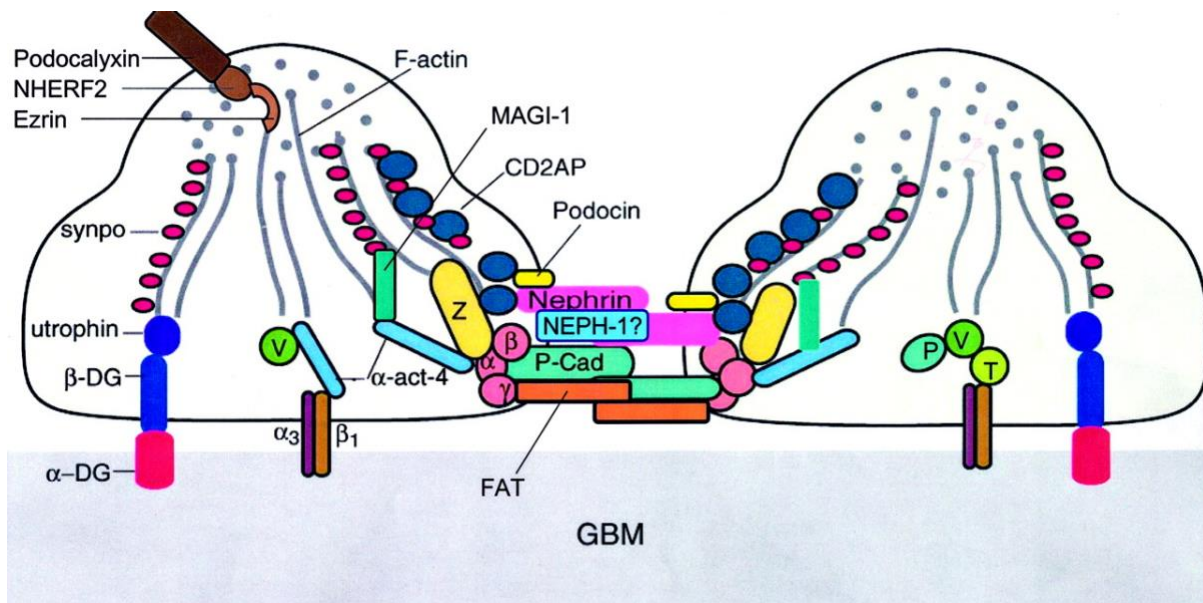


Figure 2: Schematic showing the slit diaphragm, focal adhesions, and actin regulatory proteins in podocytes. The actin cytoskeleton is the common downstream pathway that receives signals from the apical, lateral (slit diaphragm) and basal domains (where the focal adhesions link the podocyte to the GBM). This schematic shows several cytoskeletal proteins in this study: P- paxillin, V- vinculin, T- talin, and $\alpha_3\beta_1$ integrin chains. This figure is adapted from [Mundel, P. and S.J. Shankland, *Podocyte biology and response to injury*. J Am Soc Nephrol, 2002. 13(12): p. 3005-15., License ID: 1252007-3] [27].

1.2 Podocyte cytoskeleton

1.2.1 Actin cytoskeleton

The organisation of the podocyte cytoskeleton relies on the interplay between proteins, in particular actin, a 42 kDa globular protein that polymerizes into filaments of various organisations (**Figure 3**) [4, 28]. Actin filaments are organised into branched and crosslinked networks, or they can be aligned into parallel bundles [4]. This network of crosslinked filaments is interspersed with myosin IIA-containing contractile fibers which are found within contractile bundles that connect the cell cytoskeleton to the underlying extracellular matrix [20, 28]. The contractile bundles generate tension on the non-contractile actin filaments within the podocyte foot processes to anchor the cells to the basement membrane against fluid flow [29]. This mechanism is thought to be responsible for altering foot process arrangement and is essential to maintain the space between foot processes, thus allowing efficient filtration [20].

Actin polymerization is a highly dynamic process that is regulated by the continuous assembly and disassembly of actin filaments by actin-binding proteins (**Figure 3**) [8]. During foot process effacement, the actin cytoskeleton undergoes extensive rearrangement and is pulled closer to the GBM [4, 20]. It has been suggested that after injury, myosin IIA-containing contractile fibers redistribute the major processes and cell body to the basolateral aspects of the cell adjacent to the GBM [29].

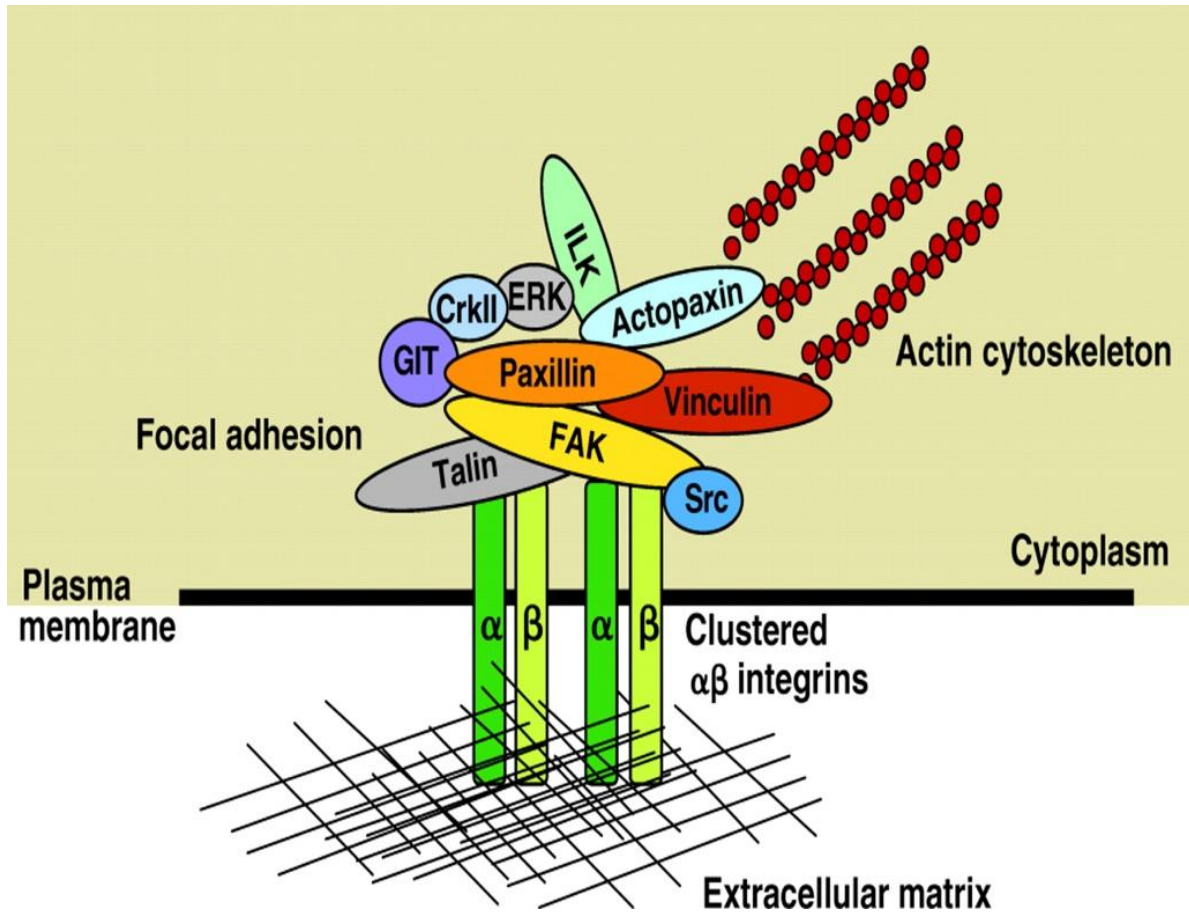


Figure 3: Focal adhesions provide both a structural and signaling link between the extracellular matrix and the actin cytoskeleton. Cell adhesion to the extracellular matrix, via transmembrane integrin $\alpha\beta$ heterodimers, leads to integrin activation and the recruitment of numerous intracellular proteins to the plasma membrane. This figure has been adapted from [Deakin, N.O. and C.E. Turner, *Paxillin comes of age*. J Cell Sci, 2008. 121(Pt 15): p. 2435-44., License ID: 1252007-4][30].

1.2.2 Focal adhesion complexes

Focal adhesions are multiprotein structures that link the intracellular cytoskeleton and the extracellular matrix (ECM) outside of the cell (**Figure 3**) [31]. Focal adhesion complexes change in number, size, and protein composition in response to the force they experience resulting in regulation of cell migration and cell adhesion. Focal adhesion assembly and maturation are highly dynamic processes which are initiated by changes in force generated within the cytoskeleton or ECM [32]. There have been recent attempts to characterise the role of small and large focal adhesions. Large focal adhesions bind strongly to the extracellular matrix and transduce force on stress fibres and are therefore more compatible for anchorage [33, 34]. On the other hand, smaller adhesions are short-lived and mediate traction forces for cell migration [33, 34]. Cells expressing a phosphomutant of paxillin had larger adhesions than control cells which adhered greatly to the ECM [35]. In other studies, drugs were used to inhibit Rac activity, which also resulted in larger focal adhesions and a greater number of focal adhesions within cells [36].

In podocytes, focal adhesion complexes provide physical linkage of podocytes to the underlying GBM and also function as signalling hubs by coordinating the recruitment of other proteins resulting in assembly and disassembly of adhesion structures (**Figure 2**) [37]. Podocyte foot processes contain several adhesion proteins which interact to anchor the podocyte to the extracellular matrix [38].

1.2.3 Integrin

Integrins, the main transmembrane receptor glycoproteins, connect the ECM to the cellular actin cytoskeleton (**Figure 3**). In podocytes, the laminin-binding $\alpha_3\beta_1$ integrin heterodimer is

the principal form of integrin in the complex and is critical in maintaining the glomerular filtration barrier [39]. Genetic deletion of β_1 or α_3 integrins result in lethal proteinuria and death in mice and human mutations encoding α_3 result in severe congenital nephrotic syndrome [40-42]. Inactivation of the integrins, through targeted mutation of α_3 or deletion of β_1 integrin genes, results in podocyte effacement and kidney failure in newborn mice [40, 43].

Integrins are bidirectional signalling molecules with no intrinsic kinase functions. However, they interact with signalling proteins, kinases, phosphatases, and adaptor proteins which all transmit signals from the cell cytoskeleton to the ECM and vice-versa to uphold the integrity of the podocyte foot processes [24]. Actin fibers are linked to focal adhesions through various focal adhesion protein complexes which contain paxillin, vinculin and talin [44]. On the cytoplasmic side, integrins interact with these protein complexes to facilitate and mediate the connection between ECM and the actin cytoskeleton [45-47].

1.2.4 Focal adhesion proteins

Upon integrin activation, there are numerous proteins that are recruited from the cytosol into the focal adhesions [48]. Chief among them are the adaptor proteins - noncatalytic molecules that contain one or more binding domains that mediate multiple protein interactions [38, 49]. Several adaptor proteins have been identified as essential for maintaining the actin cytoskeleton in foot processes and upholding podocyte structure [38]. In this study, we examined the interactions of paxillin, vinculin, and talin within focal adhesion complexes in GECs.

Paxillin, an adaptor protein with a size of 70-kDa, is one of the first proteins to be recruited to focal adhesions in the podocyte in a tyrosine phosphorylation-dependent manner [24, 31]. Paxillin is described as a multidomain scaffold protein which facilitates the efficient recruitment and interaction of other intracellular focal adhesion proteins within focal adhesion complexes [30]. Paxillin provides docking sites for other proteins to facilitate the assembly of multiprotein complexes [50]. Paxillin communicates directly with the transmembrane integrin via its Lin11, Isl and Mec-3 (LIM) domain at its C-terminus and binds to the tail domain of the vinculin protein complex [51]. The vinculin tail domain binds directly with actin filaments, therefore paxillin can indirectly mediate control of the actin cytoskeleton [31, 52].

Vinculin is another adaptor protein which is found both in focal adhesions as well as at cell-cell junctions and is comprised of an N-terminal head domain and a C-terminal tail domain [53]. Upon recruitment to focal adhesions, vinculin undergoes conformational changes, exposing its binding sites to talin, α -actinin and paxillin [52]. Vinculin activation leads to talin binding which results in integrin clustering, and subsequent recruitment of focal adhesions. Vinculin links integrins with protein complexes involved in actin polymerisation including Rho-A associated protein kinase ROCK, which induces stress fiber and focal adhesion formation. This interaction promotes myosin II activity and increases foot process contractility [54].

For vinculin to drive the formation of focal adhesions (FAs), it must interact with talin. The vinculin-talin interaction leads to the highly efficient recruitment of paxillin independently of the vinculin-paxillin binding site [55-57]. The vinculin head mediates growth of cell-matrix adhesions thereby regulating integrin dynamics and clustering while the vinculin tail regulates actin-binding and thus mediates the mechanotransduction machinery [55]. Podocytes from vinculin knockout mice had increased focal adhesion sizes as well as increased cell migration leading to unstable focal adhesions [53]. Podocyte-specific knockout of vinculin resulted in mild foot process effacement and proteinuria which was worsened with kidney injury induced by lipopolysaccharide treatment [53].

Talin is a large 270 kDa dimeric adaptor protein found in focal adhesions which is indispensable for linking integrin and the actin cytoskeleton [58]. There are two isoforms of mammalian talin: talin1 which is ubiquitously expressed and talin2 which is localised in striated muscle and in the brain [59]. Talin consists of an N-terminal FERM head domain, with four subdomains, that is connected to its large C-terminal flexible rod domain via a linker which contains which contains a calpain-II cleavage site [59, 60]. The rod domain contains bindings sites for actin, integrins, and vinculin [1, 61]. Recent studies have shown that cells lacking talin1 were noted to have reduced cell adhesion, spreading, and migration [62].

Talin is localized to the basal aspect of the podocyte and binds to the cytoplasmic tail of β_1 integrin to subunit to activate integrin [63]. Podocytes lacking talin notably had reduced cell adhesion, cell spreading and migration [58]. Talin-null podocytes also had a reduction in β_1

integrin activation as well as a reduced expression of focal adhesions [58]. Podocyte specific deletion of talin in mice resulted in severe proteinuria and foot process effacement resulting in severe kidney failure when compared with controls [58]. Thus, talin is indispensable for integrin-dependent adhesion of podocytes in the GBM.



Figure 4: Structure of SLK molecule (1204 amino acids) showing the kinase domain, phosphorylation sites and coiled-coil (CC) domain. This figure has been adapted from Luhovy, A.Y., A. Jaber, J. Papillon, J. Guillemette, and A.V. Cybulsky, Regulation of the Ste20-like kinase, SLK: involvement of activation segment phosphorylation. *J Biol Chem*, 2012. 287(8): p. 5446-58. [64].

1.3 SLK

1.3.1 *SLK structure*

The Ste20-like kinase, SLK, is a serine/threonine protein kinase that regulates organ development, cell migration, cytokinesis and cytoskeletal structure, via phosphorylation of substrate proteins [44]. SLK is classified as a group V germinal center kinase and is comprised of 1235 amino acids with a catalytic N-terminal kinase domain and a coiled-coil C terminal domain [44, 65]. The N terminal domain is the site of kinase regulation and contains the phosphorylation sites Threonine-183 and Serine-189 [64-66]. The coiled coil regions in the C domain facilitate dimerization of the SLK molecule which enhances kinase activity [64, 67].

1.3.2 *SLK activation and function*

Slk is activated by homodimerization of SLK monomers at the coiled-coil C terminal domains, which induces the phosphorylation of T183 and S189 [67]. SLK has been found to have diverse physiological functions [44]. SLK is essential in embryogenesis as global deletion was found to be lethal in mice with severe placental and tissues defects at embryonic day 12 and with death on embryonic day 14.5 [68]. Overexpression of SLK in various cell lines results in rapid disassembly of actin stress fibers and cell death [69]. In vitro studies show that SLK activity induces stress fiber disassembly as well as interacts with multiple cytoskeletal proteins [70-73].

1.3.3 *SLK Activity in the kidney and in podocytes*

SLK is richly expressed in the podocytes as well as tubular epithelial cells [24, 74]. In cultured podocyte and renal tubular cells, ischemia-reperfusion activates SLK along the p38

kinase pathway resulting in apoptosis [75]. It was shown that podocyte overexpression of SLK in transgenic mice induced damage of GECs and resulted in glomerular injury and significant proteinuria [76]. The glomeruli had fewer podocytes, with effaced foot processes and vacuolated cell bodies.

Adriamycin is a powerful podocyte toxin that induces actin fiber depolymerization in GECs and thereby disrupts their normal morphology and function [77]. *In vivo*, it induces proteinuria and foot process effacement. Adriamycin-induced nephropathy is a reproducible model of human FSGS, and is characterized by glomerulosclerosis, tubulointerstitial inflammation and fibrosis [78]. It has been proposed that Adriamycin disrupts cytoskeletal dynamics and protein production [79, 80].

Recent studies have shown that mice with podocyte-specific deletion of SLK develop albuminuria that develops at 4-5 months of age [74]. In an Adriamycin nephrosis model, SLK deletion significantly worsened albuminuria *in vivo*, increased ECM deposition and sclerosis in glomeruli [81].

1.3.4 SLK effect on focal adhesion complexes

Several substrates of SLK mediate cell motility and adhesion. SLK phosphorylates ezrin (a protein that interacts with F-actin and the plasma membrane) at the site T567 which localizes ezrin to the apical membrane of the podocyte foot processes [74, 82]. The phosphorylated ezrin forms a complex with podocalyxin and the Na⁺/H⁺ exchanger regulatory factor (NHERF2) which connects to F-actin to maintain cellular polarity and podocyte structure [67, 74]. Deletion of SLK was also found to reduce the colocalization of ezrin and podocalyxin in

the glomerulus resulting in cytoskeletal changes due to a reduction in F-actin [81]. The reduction in F-actin alters the shape of GECs which subsequently impairs cell adhesion to the ECM (i.e., podocyte adhesion to the GBM [83].) Thus, ezrin serves to link membrane proteins to the actin cytoskeleton in order to regulate cell adhesion [84].

Foot process effacement involves firm adhesion of GECs to the underlying GBM [22]. Through adhesion and motility assays, our lab has demonstrated that depletion of SLK increased GECs' adhesion to the GBM as well as significantly reduced GEC migration which can contribute to foot process effacement in vivo [67, 74]. Therefore, SLK may regulate downstream interactions within focal adhesion complexes for cell adhesion and migration.

Finally, SLK was shown to phosphorylate paxillin at serine-250 on its LD3 domain resulting in regulation of focal adhesion turnover and efficient cell migration [73]. Expression of a phospho-inactivating mutation of paxillin, S250T, abolished phosphorylation by SLK resulting in stabilized focal adhesions and impaired cell migration. Deletion of SLK in skeletal muscle impairs myofiber stability and function due to mislocalization of FAK and paxillin resulting in muscle weakness in mice. In *Drosophila*, the SLK homolog SLIK phosphorylates talin1 on threonine-152, and this phosphorylation is crucial for strong muscle attachment. Thus, SLIK was proven to be a modulator of adhesion turnover and cell migration [73].

Chapter 2: Rationale and Hypothesis

Rationale

Previous work has shown that phosphorylation of ezrin by SLK regulates podocyte structure, most likely via protein-protein interactions at the apical membrane. An outstanding question is whether there are other substrates of SLK that may also be involved in the regulation of podocyte structure and/or interactions with the GBM. SLK (or its *Drosophila* homolog SLIK) has been reported to interact with several proteins in focal adhesions, including paxillin and talin. Paxillin houses docking sites for vinculin, a cytoplasmic protein essential to maintaining glomerular barrier integrity [53]. It is reasonable to propose that SLK deletion will disrupt paxillin regulation leading to loss of integrity of the podocyte cytoskeleton and podocyte adherence to the glomerular basement membrane. SLIK was found to phosphorylate talin-1 at T152 in *Drosophila* and is crucial for muscle attachment [85]. It is also reasonable to further characterize the role of SLK in phosphorylating other focal adhesion proteins in the glomerulus, such as talin. Vinculin has binding sites for paxillin, talin, and actin stress fibres, thus providing indirect linkage of integrins to the actin cytoskeleton [55, 86]. We also anticipate that SLK deletion will disrupt vinculin distribution if paxillin is mislocalised.

Investigating the effect of SLK regulation on the actin cytoskeletal structure in podocytes and focusing on paxillin, vinculin and talin distribution within focal adhesions, will provide a better understanding of the molecular pathways causing glomerular injury and provide a framework for therapeutic interventions.

Hypothesis

We hypothesize SLK is a key regulator of focal adhesion complex dynamics and that SLK deletion will alter the number, size, and adhesion area of paxillin, vinculin and talin and thereby lead to a collapse of the actin cytoskeleton in podocytes.

Chapter 3: Materials and Methods

3.1 Antibodies and reagents:

Primary antibodies used were as follows: Mouse anti-vinculin IgG (clone V9131) (55 mg/mL in ascitic fluid), rabbit anti-paxillin (SAB4502553) (1 mg/mL), and rabbit anti-actin IgG (A2066) (0.8 mg/mL) were from Sigma-Aldrich (St-Louis, MO). Mouse anti-human talin-1 IgG (clone 97H6) (1 mg/mL) was purchased from Bio-Rad Laboratories (Mississauga, ON). Rabbit anti-nephrin antiserum was kindly provided by Dr. Tomoko Takano (McGill University). Fluorescein isothiocyanate FITC- conjugated AffiniPure Goat anti-Rabbit IgG (#111-095-003) (1.5 mg/mL), Rhodamine-conjugated AffiniPure Goat anti Mouse IgG (#415-505-1) (1.5 mg/mL), peroxidase-conjugated AffiniPure sheep-anti mouse IgG (#515-035-003) (0.8 mg/mL), and peroxidase-conjugated AffiniPure goat anti-rabbit IgG (#111-035-003) (0.8 mg/mL) were purchased from Jackson ImmunoResearch (West Grove, PA).

Cells were cultured and maintained in K1 medium (Dulbecco's Modified Eagle Serum, Ham F-12 nutrient mixture; Wisent Inc. (St. Jean Baptiste, Quebec) with 5% NuSerum (Corning Inc., Bedford, MA) and 0.5% hormone mixture as previously characterized by the Cybulsky lab [66]. Hank's Balanced Salt solution was purchased from Wisent Inc. PureCol type 1 collagen solution (3 mg/mL) was purchased from Advanced BioMatrix (Carlsbad, CA). Cell culture plates were purchased from Corning Inc. Doxycycline hyclate (Adriamycin) (4 mg/mL) and bisBenzimide H 33342 trihydrochloride (Hoechst) (1 mg/mL) were purchased from Sigma-Aldrich. Aqua-Mount mounting medium was purchased from Lerner Laboratories (Kalamazoo, MI). The protease cocktail inhibitor, bovine serum albumin (BSA), Bradford reagent and Triton X-100 were purchased from BioShop (Burlington, ON).

Enhanced chemiluminescence (ECL) detection reagent was purchased from Bio-Rad Laboratories.

3.2 Generation of SLK knockout (KO) glomerular epithelial cell clones:

The SLK cell clones were previously generated in the Cybulsky lab [81]. Briefly, glomeruli from SLK^{flox/flox} mice (see below) were harvested, plated on collagen-coated plates, and incubated at 37°C. Outgrowths of GECs were immortalized using a lentivirus-containing a temperature-sensitive simian virus 40 antigen (SV40). This SV40 antigen allows for cell proliferation at 33°C, while at 37°C proliferation ceases and cells differentiate. Cells were moved to 33°C to allow for clonal expansion. Selection of clones was carried out following addition of puromycin. Cells which did not incorporate SV40 did not survive puromycin selection while cells containing SV40 continued to grow at 33°C. GECs were characterized by expression of podocyte differentiation markers (WT1, nephrin and synaptopodin). To delete SLK, GECs were transduced with tamoxifen-inducible Cre recombinase and mCherry. Highly fluorescent cells expressing mCherry (which contain a deletion of SLK) were separated by fluorescence-activated cell sorting (FACS) and termed SLK KO cells. Untransduced cells were used as the GEC control cell line. Polymerase chain reaction (PCR) and immunoblotting were used to confirm deletion of SLK. The expression of SLK in control and KO GECs was characterised and published previously [81].

3.3 Cell Culture:

SLK KO and control GECs were used for *in vitro* experiments and were cultured in K1 medium and allowed to proliferate at 33°C until ~70% confluence. Once cells reached confluence, they were washed with Hank's Balanced Salt solution and trypsinized with

0.05% trypsin for 10 minutes. Following detachment of cells, they were resuspended in K1 medium, counted and plated for experiments: 20 000 cells were plated for immunofluorescence (IF) microscopy in 12-well plates and 150 000 cells for Western blots (WB) in 6-well plates. Cells proliferated at 33°C for one day and were transferred to 37°C for differentiation for another day. In drug experiments, selected cells were treated with 0.125 µM Adriamycin (doxorubicin) in fresh medium creating untreated and treated KO and control cells. Medium was replaced in wells containing untreated cells. Cell lines used in IF and WB experiments were between passage 20 and 50.

3.4 Measurement of Adriamycin cytotoxicity:

To determine the optimal concentration of Adriamycin treatment for GECs, we performed a crystal violet assay. We plated control GECs in a 12-well plate as above and treated each well with varying concentrations of Adriamycin (0.03, 0.07, 0.125, 0.25, 0.5 µM). Wells were washed twice with 1 mL of ice-cold phosphate buffered saline (PBS). Cells were fixed with 1 mL of ice-cold methanol and placed on ice for 10 minutes. The methanol was aspirated, and each well was incubated with 1 mL of 0.5% crystal violet solution (0.5 g crystal violet, 25 mL methanol and 75 mL of distilled water) at room temperature for 10 minutes. Wells were then carefully rinsed with distilled water and allowed to dry overnight. The plates were visually examined the following day. Concentrations greater than 0.125 µM were found to be toxic to cells.

3.5 Generation and treatment of SLK KO mice:

The podocyte-specific SLK KO mice were generated previously in the Cybulsky lab [74]. Cre recombinase technology, with podocin as the promoter, was used to delete exons 3-6 of the *Slk* gene resulting in SLK KO mice (SLK^{flox/flox};Cre/+) mice. SLK^{flox/flox};+/+ mice were the control mice. Adriamycin was administered to mice at a dose of 12-18 mg/kg intravenously via the tail vein [81]. Four weeks after treatment, kidneys were collected, and glomeruli harvested for microscopy. Animal protocols were approved by McGill University Animal Care Committee.

3.6 Immunofluorescence (IF) microscopy

GECs: Coverslips were placed into wells of a 12-well plate. Coverslips were washed twice with 70% ethanol, followed by Hank's Balanced Salt Solution (HBSS), and coated with 1 mL of collagen (1:10 dilution of original stock) for one hour at room temperature. GECs were counted using a hemocytometer and 20 000 cells were plated in each well. The cells were allowed to proliferate for one day at 33°C, then switched to 37°C to differentiate for 24 hours. Selected wells were incubated with Adriamycin for 24 hours. The medium was then aspirated, and coverslips were washed three times in PBS. For paxillin-vinculin double staining, GECs were fixed in 4% paraformaldehyde (PFA) for 15 minutes, rinsed three times in PBS and permeabilized with 0.5% Triton X-100 in PBS with 3 mM MgCl₂ for five minutes. For talin staining, the cells were fixed and permeabilized with ice-cold methanol for 15 minutes. The cells were then blocked for 1 hour in 3% bovine serum albumin (BSA) and incubated with primary antibodies overnight at 4°C. Primary antibody dilutions were as follows: rabbit anti-paxillin (1:500), mouse anti-vinculin (1:1200) and mouse anti-human talin-1 (1:750). Coverslips were washed three times in PBS, and then incubated with

fluorophore-conjugated secondary antibodies at 22°C for 1 hour. Secondary antibody were used a dilutions of 1:1000 (Fluorescein isothiocyanate FITC- conjugated AffiniPure Goat anti-Rabbit as well as Rhodamine-conjugated AffiniPure Goat anti Mouse). Coverslips were washed three times in PBS and cell nuclei were stained with 1 mL of Hoechst H33342 (1 ug/mL) for 30 minutes. Non-immune IgG replaced the primary antibodies in control experiments. Finally, coverslips were washed three times in PBS and were mounted on slides with a drop of Aqua-Mount mounting medium and kept in the dark overnight at room temperature. Images for the cultured cells were acquired using a Zeiss AxioObserver fluorescence microscope and captured with Zeiss AxioCam MRm. Images were captured at a 63x magnification.

3.7 Kidney sections: Kidney poles were frozen in isopentane and stored at -80°C [81]. Cryostat sections were cut and fixed in 4% PFA for 15 minutes, followed immediately by antigen retrieval: 10 mM sodium citrate (pH 6) for 8 minutes at 100°C. Slides were placed at 22°C to cool down, then washed in PBS for 5 minutes and blocked with 5% BSA for 1 hour. The slides were incubated with primary antibodies ((cocktail of mouse anti-human talin-1 (dilution of 1:200) and rabbit anti-nephrin serum (dilution 1:200)) at 4°C overnight. The slides were washed three times with PBS and incubated with secondary antibodies with the same dilutions as the GECs. Nuclei were stained with Hoechst H33342 (1 ug/mL). Slides were mounted with a drop of Aqua-Mount and kept in the dark overnight at room temperature. Images of glomeruli were acquired using the Zeiss Axio Observer Z1 LSM780 laser scanning confocal microscope using the same settings for all experiments. Images were captured at a 40X magnification.

3.8 Image Analysis

Focal adhesion complexes were analyzed and quantified using captured images of the stained cultured cells and NIH ImageJ software. Color photographs were split into 3 separate channels and converted to grayscale. Cell contours were selected using the freehand tool on grayscale images, and the area of the cross-section was measured. Image histogram plots were obtained, representing the range of pixel brightness values in each image. Threshold intensity was set at the end of the histogram declining slope (thereby only including the brightest fluorescent signals and omitting cellular features and background). Previous studies of focal adhesion complexes demonstrated that most focal adhesion complex protein particles are between 0.2-10 μm^2 [86]. We initially analyzed particles between 0.2-2 μm^2 , 2-4 μm^2 , 4-6 μm^2 , 6-8 μm^2 and 8-10 μm^2 for paxillin, vinculin and talin. In our study, almost all particles were found between 0.2-4 μm^2 , with the large majority found between 0.2-2 μm^2 (small adhesion proteins) across the three proteins. Hence, we were able to divide focal adhesion particles into small (0.2-2 μm^2) and large (2-4 μm^2) particles. The number of particles as well as the size of each individual particle were captured. Second, the total cross-sectional area of the particles whose areas fell within this set range was measured. The adhesion area of the small and large focal adhesion protein particles was determined by dividing the total cross-sectional area of the small and large particles by the total cross-sectional area of the cell.

To measure the colocalization of talin with nephrin in mouse kidney sections, glomeruli were contoured, and threshold intensity of each channel was measured as above. Results were normalized per 1000 μm^2 of cell area. Colocalization of the thresholded images in both

kidney sections and cultured cells was determined using the JaCOP plugin in ImageJ, which calculated the Pearson's and Manders' overlap coefficients.

3.9 Western blotting/Immunoblotting

GECs were prepared and treated as described above. Cells were washed three times with PBS. Lysates were harvested by scraping cells from culture plates using 150-200 μ l of 1x lysis buffer containing 1% Triton X-100, 125 mM NaCl, 10 mM Tris (pH 7.4), 1 mM EGTA, 2 mM Na_3VO_4 , 10 mM sodium pyrophosphate, 25 mM NaF, and 50 μ l protease inhibitor cocktail. Lysates were centrifuged at 15 000 RPM for 15 minutes at 4°C and collected in separate Eppendorf tubes. The protein content of the samples was quantified using a Bradford's protein assay, and samples were adjusted to equivalent protein concentrations. Lysates were dissolved in 3x Laemmli buffer and boiled at 95°C for 5 minutes. Lysates were separated by SDS-PAGE on a 7.5% acrylamide gel for 45 minutes at 200 V, and then transferred to polyvinylidene difluoride membranes via BioRad transblot system (25 V for 20 minutes). Membranes were blocked for 2 hours in blocking buffer (10mM Tris, pH 7.5, 50 mM NaCl, 2.5 mM EDTA, and 0.05% Tween 20 with 5% BSA) on a rotating wheel, and then incubated with primary antibody overnight at 4°C under the same conditions. Dilutions for the primary antibodies used were as follows: rabbit anti-paxillin (1: 1000), mouse anti-vinculin (1: 5000), mouse anti-human talin-1 (1: 2500), rabbit anti-actin (1: 5000). The following day, membranes were washed 3 times for 5 minutes in 10mM Tris, pH 7.5, 50 mM NaCl, 2.5 mM EDTA, and 0.05% Tween 20 (TBST) buffer and incubated with horseradish peroxidase-conjugated secondary antibody (dilutions of 1: 10 000) for one hour at 22°C. Membranes were washed three times in fresh TBST and exposed using enhanced

chemiluminescence, such that signal intensities of protein bands were within a linear range. Quantitative densitometry of protein bands was done using ImageJ. The densities of all target proteins and actin (housekeeping protein) bands were measured in each lane. The density of each band of interest was normalised to the density of the actin band in the same sample. Results were expressed in arbitrary unit.

3.10 Statistics

In all experiments, data are presented as mean \pm standard error of the mean (SEM). One way ANOVA was used to determine significance among groups with the critical value adjusted according to the Šídák test. Statistical analyses and graphical presentation of results were performed using GraphPad Prism v9 software. P values were considered statistically significant if $P < 0.05$.

Chapter 4: Results

4.1 SLK deletion increases small vinculin, paxillin and talin particles number and decreases large paxillin particle number.

SLK activity is reported to regulate podocyte function and integrity. Previous studies suggested that SLK activity may regulate actin skeletal structure within GECs and that several SLK substrates mediate cell motility and adhesion within focal adhesion complexes [74]. Thus, we generated GECs with SLK-specific deletion and examined whether this deletion would disrupt focal adhesion interactions between paxillin, vinculin and talin *in vitro* which could explain the ultrastructural changes *in vivo*.

We used immunofluorescence microscopy to address focal adhesion particle counts after staining control and knockout (KO) GECs. We examined particle numbers, sizes, and adhesion areas of paxillin, vinculin and talin in control and SLK KO GECs as well as the colocalization of paxillin and vinculin (**Figure 5**). In **Figure 5A and C**, GECs were co-stained with paxillin (green) and vinculin (red) to examine focal adhesion particle distribution. In **Figure 5B and D**, GECs were stained with talin (red). By immunofluorescence microscopy, we show that SLK deletion induces changes in the number of small particles as well as the adhesion areas (quantification is presented below). Adriamycin is a nephrotoxin that induces glomerular injury *in vivo* and disrupts cytoskeletal structure in GECs. In podocytes, Adriamycin induces actin depolymerization and dose-dependent disassembly of focal adhesion complexes [87, 88]. We therefore examined the effects of Adriamycin treatment on vinculin, paxillin and talin particles in control and SLK

KO GECs (**Figure 5C, D**) [81]. SLK deletion decreased the number of vinculin and paxillin as well as the adhesion area in Adriamycin-treated GECs.

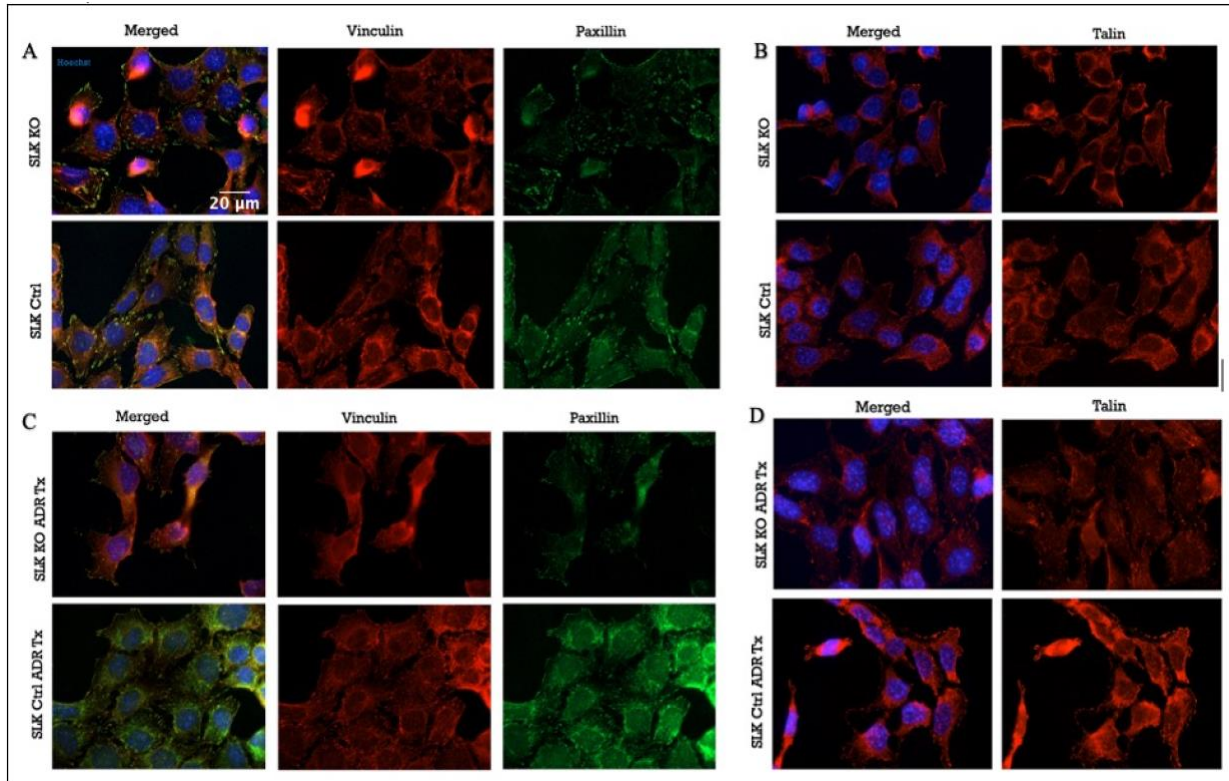


Figure 5: Representative images of immunofluorescence staining of focal adhesion proteins in Control (Ctrl) and SLK Knockout (KO) GECs. Immunofluorescence staining of (A) vinculin (red) and paxillin (green) and (B) talin (red) in untreated SLK Ctrl and KO GECs. Immunofluorescence staining of (C) vinculin (red) and paxillin (green) and (D) talin (red) in Adriamycin treated SLK Ctrl and KO GECs. Nuclei were stained with Hoechst H33342.

First, we examined the effect of SLK deletion on small and large vinculin, paxillin and talin particle number (i.e., focal adhesion particle number) using control and KO GECs (**Figure 6**). Compared with control GECs, small vinculin, paxillin and talin particle number were increased in the KO GECs (**Figure 6A**). There was a borderline increase in large talin particles in KO GECs, but this was not statistically significant ($P=0.06$). The increase in small paxillin particles was associated with a decrease in large paxillin particle number when compared with control GECs (**Figure 6B**). The total number of particles (i.e., small and large) showed a similar change as the change in small particle number for all three adhesion proteins (**Figure 6C**). Thus, SLK deletion increases the number of small vinculin, paxillin and talin particles and decreases the number of large paxillin particles in GECs.

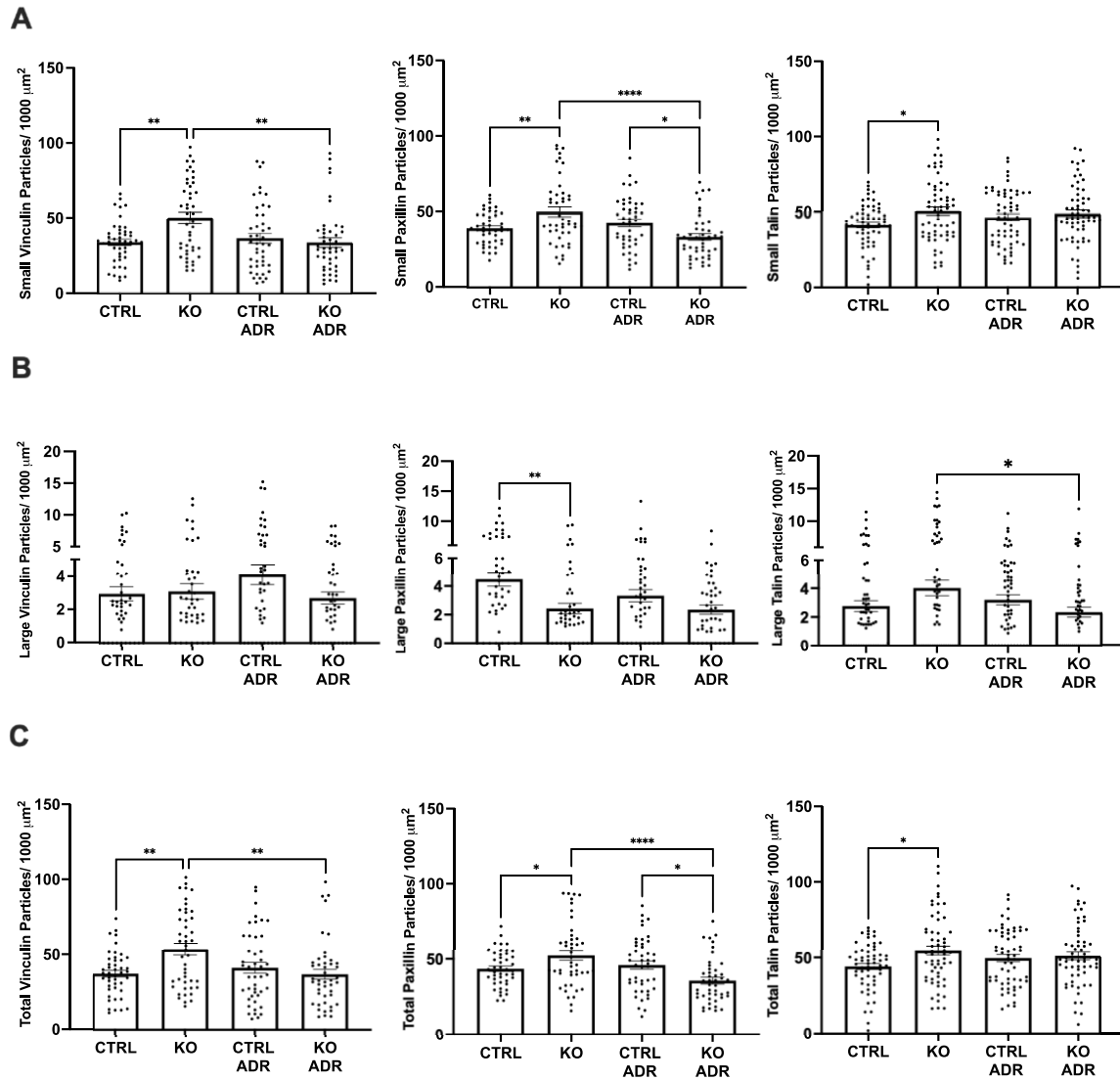


Figure 6: SLK deletion increases small vinculin, paxillin and talin particle numbers and decreases paxillin large particle number. Quantification of small (A), large (B) and total (C) number of vinculin, paxillin and talin particles in control (CU) and SLK KO GECs which were untreated or incubated with Adriamycin (ADR). (A) The number of small vinculin, paxillin and talin particles was increased in KO GECs, while Adriamycin treatment significantly decreased the number of paxillin particles in KO ADR cells. (B) There was a reduction in the number of large paxillin particles in KO GECs when compared with control and KO GECs treated with Adriamycin when compared with KO untreated. There was a

borderline increase in the number of large talin particles in the KO untreated GECs ($P=0.06$).

(C) There was an increase in the total number of vinculin, paxillin and talin particles in untreated KO GECs, while Adriamycin treatment significantly decreased the number of paxillin particles in the KO ADR cells. Data are presented as mean \pm SEM; Ordinary one-way ANOVA; * $P<0.05$; ** $P<0.01$; *** $P<0.001$; **** $P<0.0001$; (n=3 experiments; 20 cells per group per experiment).

4.2 SLK deletion increases adhesion area of small vinculin particles and large talin particles.

Next, we investigated the size of adhesion areas for small and large particles of vinculin, paxillin, and talin in control and KO GECs. Compared with control GECs, KO GECs showed an increase in adhesion area for small vinculin and large talin particles (**Figures 7A, B**). However, we observed a decrease in adhesion area of large paxillin particles in the KO GECs which was associated with a significant decrease in total adhesion area of paxillin particles (**Figure 7C**). We conclude that SLK deletion significantly increases adhesion area of small vinculin and large talin particles.

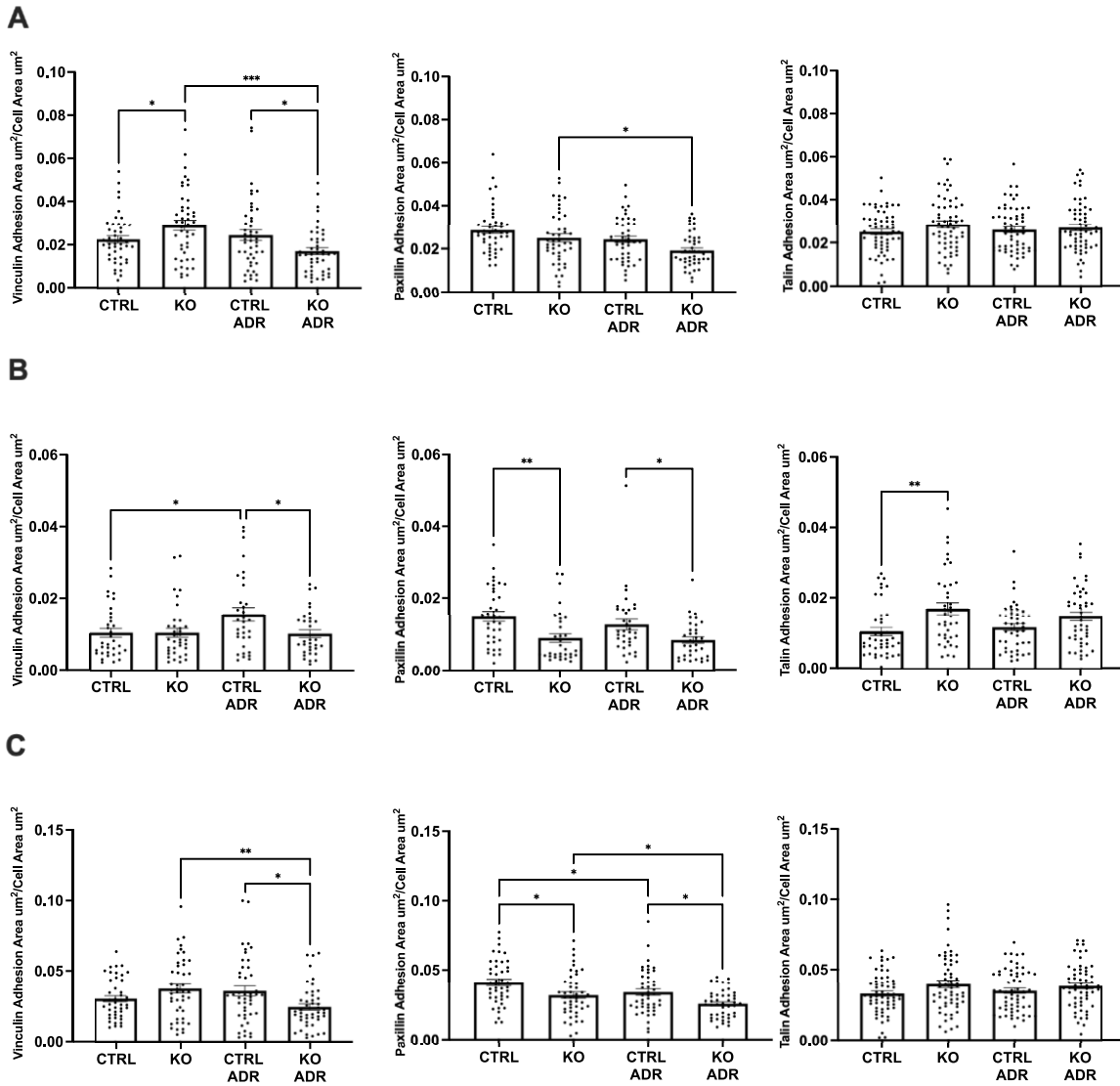


Figure 7: SLK deletion increase adhesion area of small vinculin particles and large talin particles. Quantification of small (A), large (B) and total (C) adhesion area of vinculin, paxillin and talin particles in control (CU) and SLK knockout (KO) GECs, which were untreated or incubated with Adriamycin treatment (ADR). (A) KO GECs show an increase in vinculin adhesion area of small particles and a significant decrease in Adriamycin treated KO GECs. The KO ADR GECs show a similar decrease in small paxillin particle adhesion area. (B) KO GECs showed a decrease in large paxillin adhesion area and an increase in large talin particle adhesion area. Adriamycin treatment further reduced adhesion area for both large

vinculin and paxillin particles in KO GECs. (C) KO GECs showed a decrease in total adhesion area for the paxillin particles. We observed a significant decrease in total adhesion area for vinculin and paxillin particles with Adriamycin treatment in KO GECs. Data are presented as mean \pm SEM; Ordinary one-way ANOVA; * P <0.05; ** P <0.01; *** P <0.001; **** P <0.0001; (n=3 experiments; 20 cells per group per experiment).

4.3 SLK deletion does not alter vinculin, paxillin, and talin particle size.

There were no substantial differences in the mean size of small and large particles among the three focal adhesion proteins studied (**Figure 8**), although a few differences reached statistical significance. These differences included decreases in total paxillin size in treated control GECs when compared with untreated control GECs as well as KO GECs when compared with control. We also observed a decrease in small vinculin particle size in treated knockout GECs when compared with treated control. Overall, these results indicate that deletion of SLK preserves small and large vinculin, paxillin, and talin particle size in focal adhesion complexes but induces changes in particle number and adhesion area.

4.4 SLK deletion decreases particle number and adhesion area in glomerular epithelial cells treated with Adriamycin.

Previous studies revealed that SLK KO mice were more susceptible to Adriamycin-induced glomerular injury than control mice [81]. We examined the effects of Adriamycin on adhesion proteins in cell culture which revealed a decrease small and large vinculin and paxillin particle number in Adriamycin treated KO GECs (**Figure 6**). Similarly, adhesion areas of small and large vinculin and paxillin particles decreased (**Figure 7**). Thus, we conclude that deletion of SLK decreases vinculin and paxillin particle number and adhesion areas in Adriamycin treated GECs.

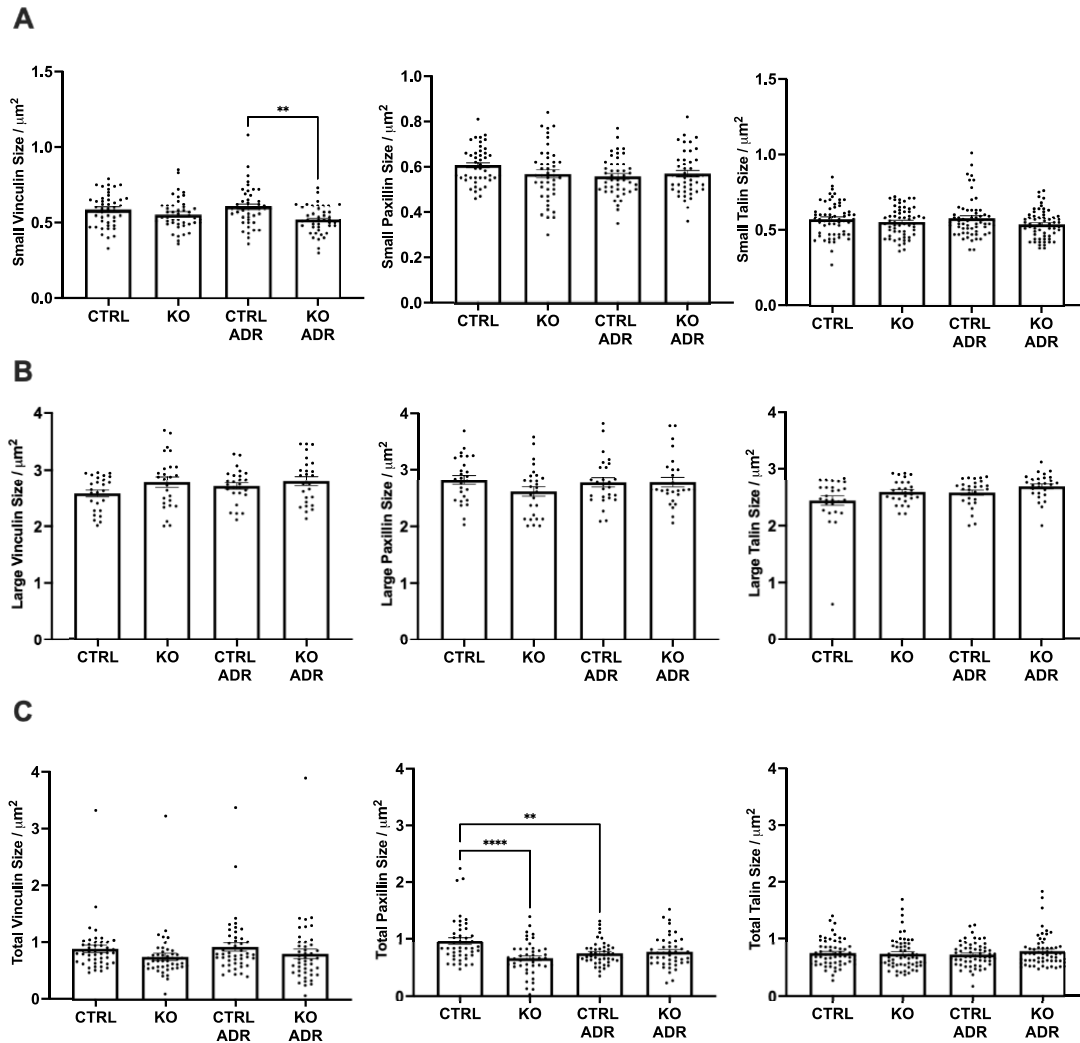


Figure 8: SLK deletion does not substantially alter small and large paxillin, vinculin and talin particle sizes. Quantification of small (A), large (B) and total (C) sizes of vinculin, paxillin and talin particles in control (Ctrl) and SLK knockout (KO) GECs, which were untreated or incubated with Adriamycin (ADR). We did not observe any significant differences in (A) small and (B) large particle sizes for all three focal adhesion proteins. (C) The total size of paxillin particles was decreased with SLK deletion and in Adriamycin-treated controls. Data are presented as mean \pm SEM; Ordinary one-way ANOVA; * $P < 0.05$; ** $P < 0.01$; *** $P < 0.001$; **** $P < 0.0001$; (n=3 experiments; 20 cells per group per experiment).

4.5 SLK deletion does not alter paxillin and vinculin colocalization.

Paxillin is phosphorylated by SLK at an early stage during the assembly of focal adhesions in fibroblasts [73]. To assess whether SLK deletion mislocalizes paxillin in GECs, we examined paxillin colocalization with vinculin. To quantify the degree of colocalization, we used Pearson's correlation coefficient and Manders' overlap coefficients (MOC). Pearson's correlation assesses overlap of the two channels (red representing vinculin and green representing paxillin) and reflects their linear relationship. The values range from -1 (perfect negative correlation) to 1 (perfect positive correlation) [89]. MOC estimates the degree of contribution (co-occurrence) of one colour channel in the colocalized area of the overall cell (i.e., fraction of one protein colocalizing with another). Manders 1 overlap coefficient (MOC1) determines green image contribution (fraction of paxillin colocalizing with vinculin) while Manders 2 overlap coefficient (MOC2) describes the contribution of the red channel (vinculin colocalizing with paxillin).

We did not observe any significant differences in colocalization of vinculin and paxillin using Pearson's correlation (**Figure 9A**). The MOC1 reveals a significant increase in paxillin particles colocalizing with vinculin in treated KO cells compared to untreated KO cells (**Figure 9B**). MOC2 also revealed significantly lower vinculin particles colocalizing with paxillin in treated KO cells than treated control cells (**Figure 9C**).

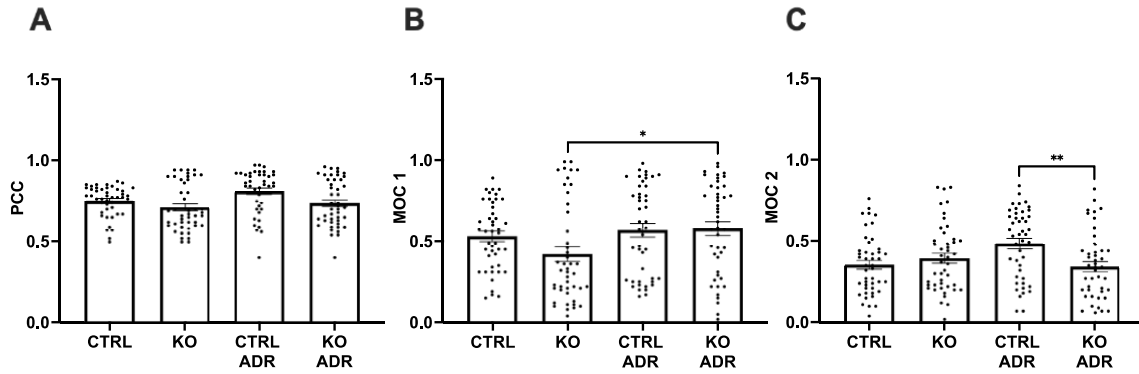
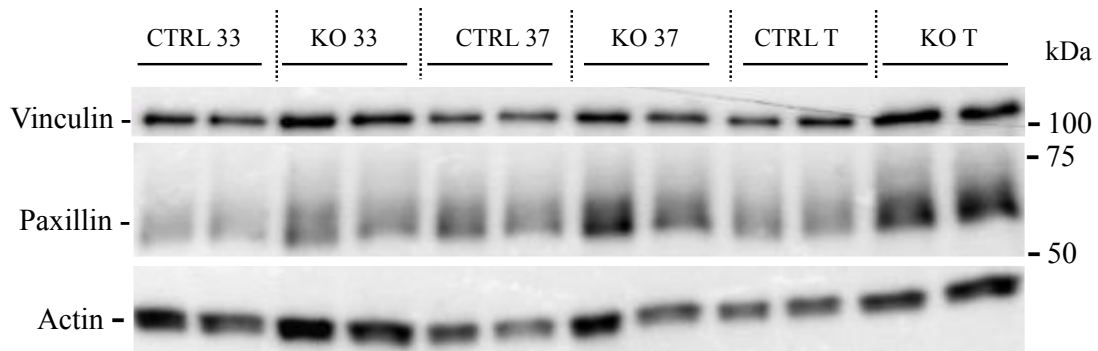


Figure 9: Effect of SLK deletion on paxillin-vinculin colocalization. Representative images are shown in **Figure 5**. *A)* There were no significant differences in the Pearson's correlation coefficient across the four groups. *B)* There was a significant increase in the MOC1 in treated KO GECs when compared with untreated KO indicating an increase in paxillin particles colocalizing with vinculin in treated KO compared to untreated KO GECs. *C)* There was a decrease in the MOC2 in treated KO compared to treated control GECs indicating a decrease in vinculin particles colocalizing with paxillin in treated KO GECs compared to treated control GECs. Data are presented as mean \pm SEM; Ordinary one-way ANOVA; * $P < 0.05$; ** $P < 0.01$; (n= 3 experiments; 15 cells per group per experiment).

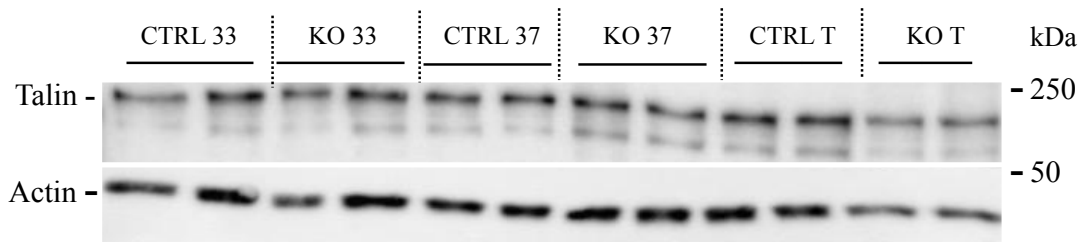
4.5 SLK deletion does not alter total expression of focal adhesion proteins.

Next, we analyzed total cellular expression of paxillin, talin and vinculin using WB analysis of whole GEC lysates. Control and knockout GECs at 33°C (proliferating), 37°C (differentiating) and Adriamycin treated GECs were blotted. Image densitometry of immunoblots revealed significant increases in paxillin expression in control and KO GECs at 37°C when compared to control and KO GECs at 33°C. Nevertheless, the results indicate that SLK deletion does not change focal adhesion protein expression in GECs (**Figure 10**).

A



B



C

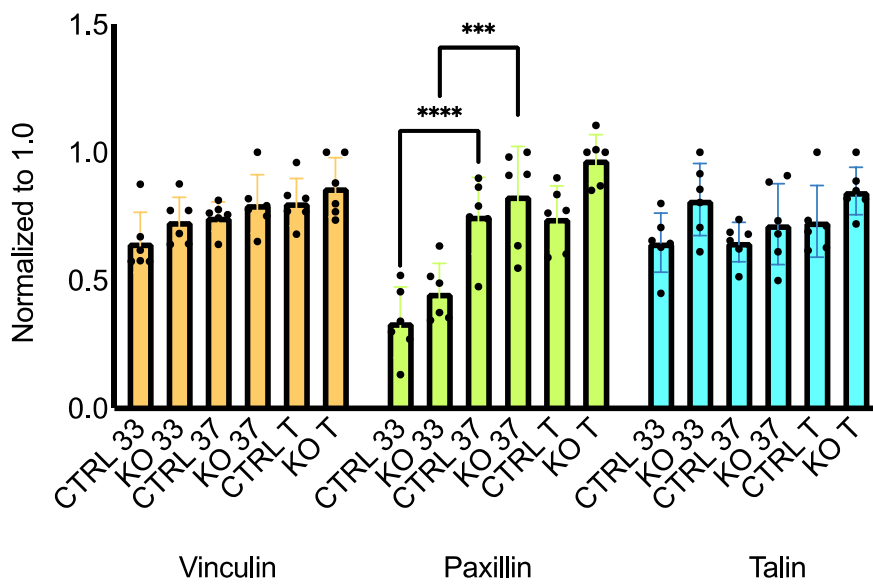


Figure 10: Immunoblot showing Control and SLK KO GECs at 33°C (proliferation), 37°C (differentiation) and with Adriamycin treatment. WB of (A) vinculin and paxillin, and talin expression in GECs at 33°C, and with Adriamycin treatment (T) at 37°C. B) Vinculin, paxillin and talin expression in GECs from A and B by image densitometry

analysis. Paxillin expression was significantly increased in Control GECs at 37°C when compared with Control GECs at 33°C. We observed a similar increase in paxillin expression in KO GECs at 37°C when compared with KO GECS at 33°C. We did not observe any significant differences in vinculin and talin expression across the 3 groups. Data are presented as mean +/- SEM; Ordinary one-way ANOVA; ***P <0.001; ****P <0.0001; (n= 3 experiments performed in duplicate).

4.6 SLK deletion increases talin and nephrin colocalization in mouse glomeruli.

Next, we conducted *in vivo* studies to examine colocalization of talin with nephrin, a component of the glomerular slit diaphragm, in control and SLK KO mice glomeruli in mice with and without Adriamycin treatment (**Figure 11**). Talin binds to the tail domain of the integrin β subunit, regulating integrin activation and function [90]. Nephrin also mediates a signalling pathway that results in activation of integrin β 1 at focal adhesions and possibly regulates podocyte adhesion to the extracellular matrix [91]. We therefore examined colocalization of nephrin with talin, to determine how SLK might affect the interaction of nephrin with focal adhesion complexes.

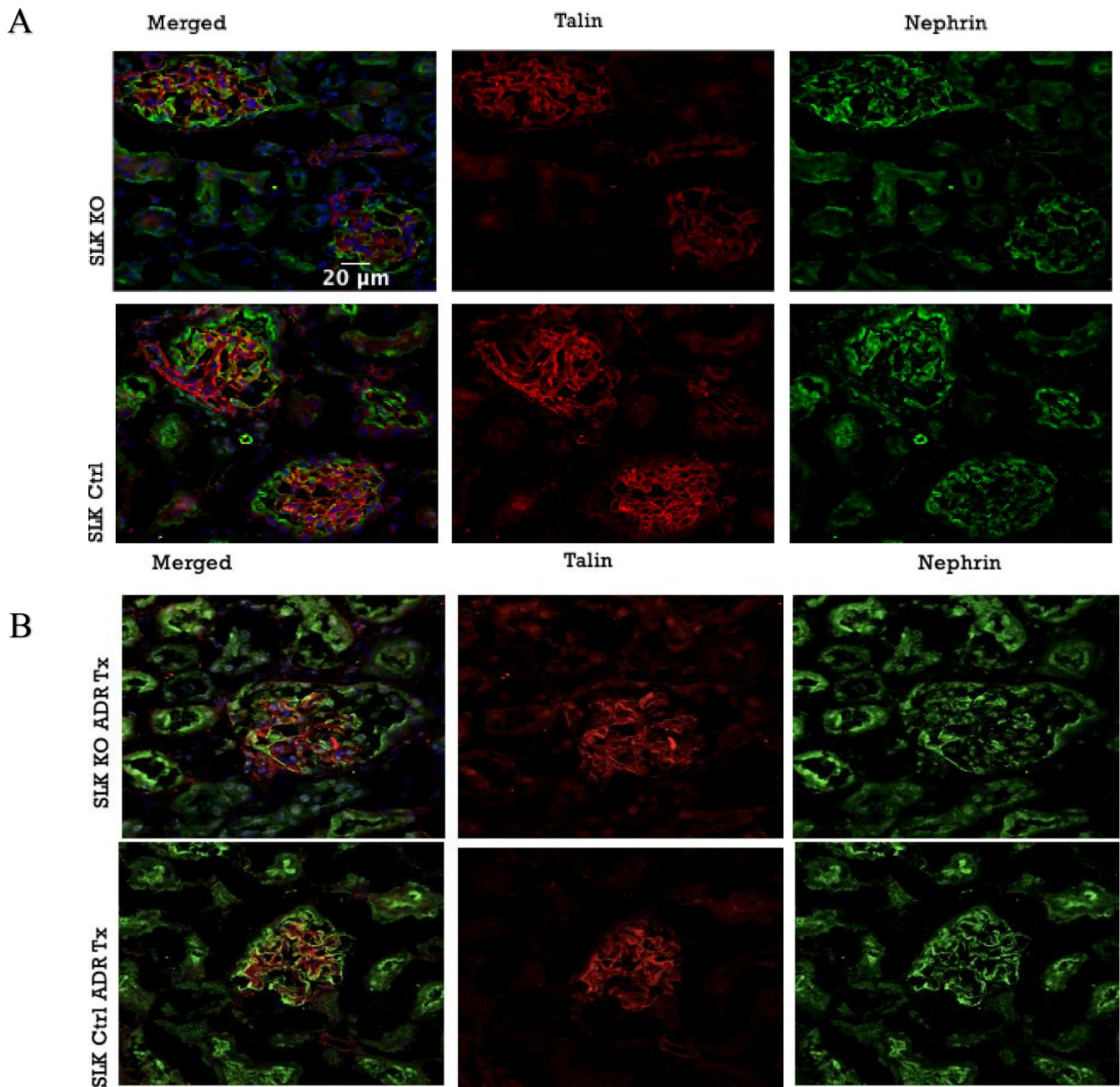


Figure 11: Representative images of talin (red) and nephrin (green) staining in (A) untreated and (B) Adriamycin treated (ADR Tx) control and SLK KO mice glomeruli sections.

Our results revealed that talin and nephrin colocalization was increased in SLK KO mice glomeruli (**Figure 12**). It is reasonable to consider that in KO mice, talin particles occupy a greater area within the glomeruli and may localise to the basolateral aspect of the podocyte where there is increased interaction with nephrin. This increase in talin-nephrin colocalization is consistent with cell culture findings of an increase in adhesion area of large talin particles. Adriamycin treatment revealed a decrease in colocalization of talin and nephrin in SLK KO mice when compared to treated controls in the Pearson's correlation coefficient as well as the MOC2 (talin colocalizing with nephrin). However, the MOC1 (nephrin colocalizing with talin) did not revealed any changes in colocalization with Adriamycin treatment across the groups. Overall, Adriamycin treatment on talin-nephrin colocalization in SLK KO mice seems to result in an overall decrease in colocalization.

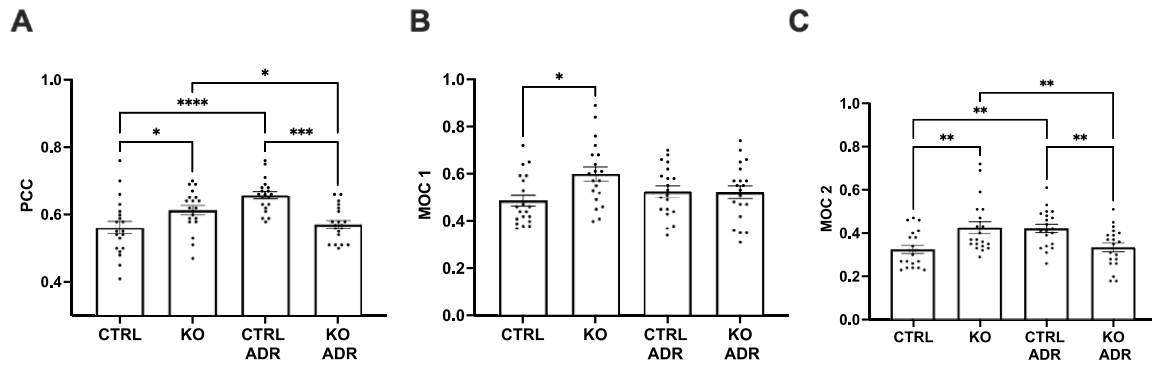


Figure 12: Deletion of SLK increases talin-nephrin colocalization. Quantification of talin-nephrin colocalization in control (Ctrl) and SLK knockout (KO) GECs, which were untreated or incubated with Adriamycin (ADR). Pearson's correlation coefficient, MOC1 (nephrin colocalizing with talin) (B) and MOC 2 (talin colocalizing with nephrin) revealed an increase in talin-nephrin colocalization in SLK KO mice glomeruli. A) Adriamycin treatment resulted in increased colocalization in control mice and a significant decrease in KO mice when compared with treated control mice. C) MOC2 also showed significantly increased colocalization in treated control mice compared to untreated control mice. Colocalization significantly decreased in treated KO mice when compared to untreated KO mice. Data are presented as mean \pm SEM; Ordinary one-way ANOVA; * $P < 0.05$; ** $P < 0.01$; *** $P < 0.001$; **** $P < 0.0001$; (20 measurements/group in 4 mice/group).

We did not observe any significant differences in talin and nephrin immunofluorescent intensity across the four groups (**Figure 13A**). Therefore, SLK deletion and Adriamycin treatment did not affect talin and nephrin expression in the glomeruli. Lastly, SLK deletion did not alter glomerular total area across all four groups (**Figure 13B**). Overall, these findings indicate that SLK deletion increases talin-nephrin colocalization in the mouse glomeruli.

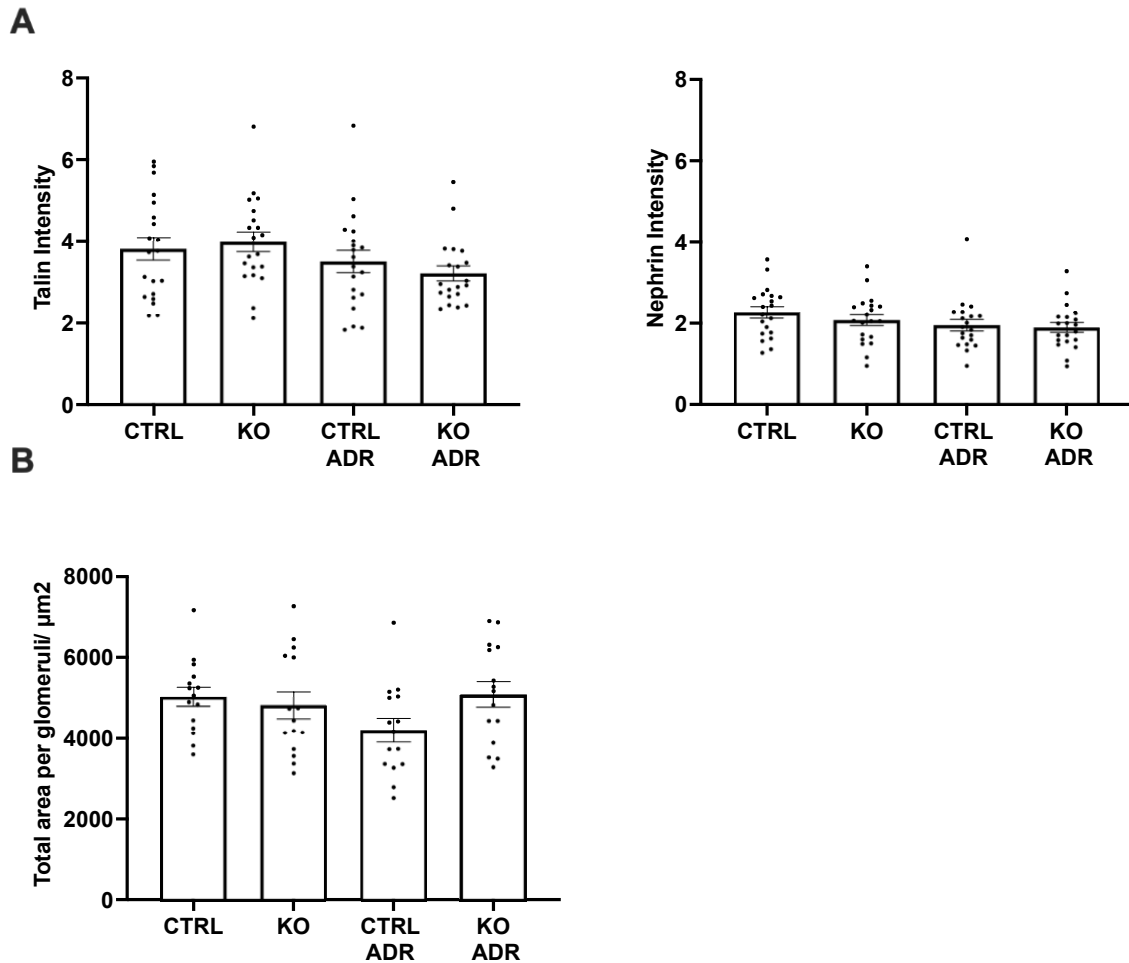


Figure 13: Deletion of SLK does not alter (A) talin and nephrin immunofluorescence intensity or (B) glomerular total area. (A) Quantification of talin-nephrin colocalization in glomeruli of control (Ctrl) and SLK knockout (KO) mice, which were untreated or incubated with Adriamycin (ADR) revealed no differences across the four groups. (B) Quantification of total area per glomeruli in each group did not reveal any differences. Data are presented as mean \pm SEM; Ordinary one-way ANOVA; 20 measurements/group in 4 mice/group.

Chapter 5: Discussion

Our results show that deletion of SLK in glomerular epithelial cells (GECs) results in changes to particle number and adhesion area of vinculin, paxillin and talin within the focal adhesions. SLK deletion also increases talin and nephrin colocalization in mice. SLK deletion decreases particle number and adhesion area in GECs treated with Adriamycin *in vitro*. The effect of Adriamycin treatment on talin-nephrin colocalization in SLK KO mice remains inconclusive.

Focal adhesions transmit forces from the matrix to the underlying cytoskeleton, resulting in changes in number, size, and composition of focal adhesion complexes due to the level and nature of the force experienced. Activation of multiple pathways results in cytoskeletal remodelling and formation of mature, focal adhesions. Previous studies have shown that loss of ROCK2 (a key regulator of cell adhesion dynamics) results in a reduction of adhesion complex turnover leading to the formation of large, stable focal adhesions [92]. Our lab has previously shown that knockdown of SLK in GECs show increased adhesion in adhesion assays [74]. Therefore, we examined small and large focal adhesion protein particles in GECs to determine whether SLK regulates size, number, and overall adhesion area of focal adhesion complexes.

Paxillin localizes to focal adhesions primarily through its LIM domain by binding to integrins (specifically $\beta 1$ integrin) [57]. Paxillin binds to the vinculin tail domain which reorganizes, recruits focal adhesions, and transmits signals to the actin cytoskeleton [93]. As SLK deletion did not alter the sizes of the focal adhesion protein particles, we analysed small and large paxillin, vinculin, and talin particle number within the GECs to determine overall differences.

When investigating the number of small particles for all three focal adhesion proteins, we found that SLK deletion increases small vinculin, paxillin and talin particle number within focal adhesions (**Figure 6**). Paxillin is phosphorylated on S250 by SLK, which induces its recruitment into focal adhesions in a FAK-dependent manner [73]. Phosphorylated paxillin binds to FAK and induces disassembly of focal adhesions [94]. Our results suggest that SLK deletion may increase unphosphorylated paxillin particle number and thereby disrupt the disassembly of focal adhesion complexes resulting in a high formation to turnover ratio.

Although not demonstrated in this study, it is plausible to consider that SLK deletion reduces paxillin phosphorylation, resulting in lower recruitment of phosphorylated paxillin within focal adhesions, and an increase in small, unphosphorylated paxillin particles. Paxillin is said to be necessary for vinculin recruitment in focal adhesions [95]. With an increase in paxillin particles within the adhesions, there may be dysregulation of adhesion disassembly, thus greater retention of vinculin and talin particles in the adhesion complexes. As expected, we found that SLK deletion increases small vinculin and talin particle numbers within the GECs as well as the adhesion area of the small vinculin particles (**Figure 6**). We can also conclude that the focal adhesions are mostly composed of small particles as seen in **Figure 6** where the graph of the total number of particles closely resembles the graph of the small particles.

It has been previously shown that SLK and talin colocalize at focal adhesions. In skeletal muscle, a conditional KO of SLK results in progressive myopathy [96]. In our study, we found that SLK deletion increased large talin particle adhesion area in GECs (**Figure 7**) and increased the colocalization of talin and nephrin in glomeruli (**Figure 12**). Mice with SLK deletion show focal foot process effacement, and in these mice, nephrin may potentially

adopt a more basolateral distribution in podocytes. Recently, Maywald et al identified Rap1 as a downstream regulator of nephrin signalling to integrin β 1 which may be essential to focal adhesion and slit diaphragm integrity [97]. Deletion of SLK may impair turnover to formation ratio in podocytes resulting in abundance of large, mature talin particles which migrate to the basal aspect of the podocyte and colocalize with nephrin, suggesting that SLK regulates the cycling of talin within podocytes and restricts it to the focal adhesion complex. This finding could be validated by colocalizing talin with β 1 integrins (basolateral podocyte proteins) in glomeruli of SLK KO mice (further discussed in Future Directions, below).

In our WB analysis we found that SLK deletion did not alter the total expression of focal adhesion proteins within the GEC lysates (**Figure 10**). There was however an increase in paxillin expression during differentiation, but the biological significance remains inconclusive. There were no significant differences in vinculin and talin expression. Therefore, SLK does not alter the overall expression of paxillin, vinculin and talin within GECs but instead regulates their distribution within the focal adhesions.

We did not observe any significant differences in colocalization of vinculin and paxillin in untreated GECs (**Figure 9**). In treated GECs, the MOC1 revealed a significant increase in colocalization in treated KO GECs compared with untreated GECs and the MOC2 revealed a decrease in colocalization in treated KO GECs when compared with untreated GECs. Though these changes reached statistical significance, the biological significance underlying these observations remains unclear.

Overall, our *in vitro* studies indicate that SLK deletion increases the number of small particles of all three focal adhesion proteins. While there was a predictable increase in the adhesion area of the small vinculin particles, there were no significant changes in the adhesion areas of paxillin and talin small particles. SLK KO GECs also had a borderline increase in large talin particles associated with a significant increase in the adhesion area of large talin particles. This may suggest that SLK may be implicated in various downstream pathways, which may directly impact the regulation of each focal adhesion protein.

Our *in vivo* studies on mouse glomeruli did not reveal any changes in fluorescent intensity of talin nor nephrin in treated nor untreated SLK KO mice (**Figure 13**). Previous studies revealed a decrease in nephrin intensity in glomeruli of Adriamycin-treated SLK KO mice [81]. This finding was not observed in our study. Increasing the number of measurements per group could have possibly yielded a significant decrease in nephrin intensity in the Adriamycin-treated SLK KO mice in the current study.

Foot process effacement has been interpreted as an adaptive response to cell injury resulting in broad and firm adhesion to the glomerular basement membrane [22]. Deletion of SLK was shown to induce ultrastructural abnormalities in mice, including widened foot processes and foot process effacement [74]. Through adhesion and motility assays, our lab has demonstrated that depletion of SLK increased the adhesion of GECs to the GBM and significantly reduced GEC migration which can contribute to foot process effacement *in vivo* [74]. This evidence supports our findings of increased cell adhesion in small vinculin and large talin adhesion areas in SLK KO GECs. Thus, SLK deletion results in increased focal adhesion area and GEC adhesion to the GBM during foot process effacement.

Throughout the experiments, we used Adriamycin to induce nephropathy in SLK control and KO mice. Podocytes undergo a change in shape and retraction of their foot processes as an early adaptive response to cell injury. This initial response results in increased adhesion to the glomerular basement membrane to prevent podocyte loss [22]. However, this initial response is limited, and the second phase of injury response results in the rearrangement of the podocyte cytoskeleton and impairment of adhesion. Adriamycin induces proteinuria *in vivo* and mice with podocyte-specific deletion of SLK showed worsened glomerular injury. SLK KO mice treated with Adriamycin may be unable to mount the same adaptive response as treated control mice, resulting in a decrease in colocalization of talin and nephrin. This may explain our findings of decreased particle numbers and adhesion areas as well as decreased talin/nephrin colocalization in treated KO GECs and SLK KO mice with Adriamycin-induced nephropathy.

5.1 Conclusion

From our *in vitro* and *in vivo* experiments, we can conclude that SLK may play a role in regulating downstream interactions within focal adhesion complexes for cell adhesion in podocytes. We demonstrated that podocyte specific KO of SLK decreases paxillin in focal adhesion complexes, potentially resulting in a dysregulation of focal adhesion disassembly, thereby disrupting the cytoskeletal architecture in podocytes. Furthermore, SLK has been implicated as a regulator of talin cycling and SLK deletion impairs talin localisation to the focal adhesion complexes and enhances colocalization of talin and nephrin *in vivo*.

5.2 Future Directions

5.2.1 Colocalization experiments between talin and $\beta 1$ integrin or $\alpha 5$ collagen

The binding of talin to the cytoplasmic tail of $\beta 1$ integrins triggers a conformational change in the extracellular domain of the integrins [17]. GECs with podocyte-specific KO of talin-1 had a modest reduction of $\beta 1$ integrin activation, reduced cell spreading and perturbation of the actin cytoskeleton [17]. Future studies in this project could involve investigating the colocalization of talin with $\beta 1$ integrins in treated and untreated SLK control and KO mice. Podocyte specific deletion of $\beta 1$ integrins in mice leads to podocyte defects and renal dysfunction at birth, underscoring the importance of $\beta 1$ integrins for maintaining the GBM [98]. Reduced expression of $\beta 1$ integrins has been noted in FSGS and several animal models of experimental glomerulonephritis [99]. Our results have shown that SLK deletion increases the colocalization of talin and nephrin. Although, we employed nephrin as a podocyte basolateral marker, the result can also be interpreted to suggest an increase in talin particles at the slit diaphragm. A future colocalization study will investigate the effects of SLK deletion on $\beta 1$ integrins, as well as colocalization between talin and $\beta 1$ integrins at the basal aspect of podocytes. This could highlight a role for SLK as an essential regulator for the interaction of integrins and focal adhesion complexes in maintaining podocyte structural integrity.

Collagen IV is a key component of all basement membranes and is encoded by six genes in vertebrates. Collagen IV forms triple helix trimers [100]. The GBM is comprised predominantly of $\alpha 3\alpha 4\alpha 5$ networks of collagen IV that contributes significantly to its structural stability and assembly [1, 101]. Defects in the $\alpha 3\alpha 4\alpha 5$ collagen IV chains result in a weak GBM which can split and have a typical thin basket-weave network appearance. Cell

adhesion to the GBM involving adhesion proteins is critical to maintaining barrier integrity. Future studies could include colocalizing $\alpha 5$ collagen with talin-1 in SLK control and KO mice to see if talin will colocalize at the basal aspect of the podocyte and how SLK deletion may alter this interaction.

5.2.2 Investigating the SLK phosphorylation of paxillin and mammalian talin in GECs

Previous studies have shown that SLK phosphorylates paxillin on its serine residue 250 in fibroblasts [73]. Similarly, the *Drosophila* homolog SLIK phosphorylates talin-1 at T152. Another future direction could include investigating the phosphorylation of paxillin and mammalian talin in GECs by SLK. Through western blot analysis and immunofluorescence, it can be confirmed whether SLK KO cells have reduced or complete loss of phosphorylated paxillin (S250). Immunoprecipitation and mass spectrometry could also be used to identify SLK-dependent phosphorylation sites on mammalian talin. Should it be found that SLK does regulate paxillin and talin phosphorylation in GECs, investigation to determine the downstream pathways disrupted by SLK deletion would elucidate other important roles of SLK in podocyte injury.

Chapter 6: References

1. Lennon, R., M.J. Randles, and M.J. Humphries, *The importance of podocyte adhesion for a healthy glomerulus*. Front Endocrinol (Lausanne), 2014. **5**: p. 160.
2. Scott, R.P. and S.E. Quaggin, *Review series: The cell biology of renal filtration*. J Cell Biol, 2015. **209**(2): p. 199-210.
3. Reiser, J., M. Altintas, K. Ulgen, D. Palmer-Toy, V. Shih, and D. Kompala, *Emerging Roles for Metabolic Engineering - Understanding Primitive and Complex Metabolic Models and Their Relevance to Healthy and Diseased Kidney Podocytes*. Current Chemical Biology, 2008. **2**: p. 68-82.
4. Sever, S., *Role of actin cytoskeleton in podocytes*. Pediatr Nephrol, 2021. **36**(9): p. 2607-2614.
5. Price, P.M., *A role for novel cell-cycle proteins in podocyte biology*. Kidney Int, 2010. **77**(8): p. 660-1.
6. Pavenstadt, H., W. Kriz, and M. Kretzler, *Cell biology of the glomerular podocyte*. Physiol Rev, 2003. **83**(1): p. 253-307.
7. Tian, X. and S. Ishibe, *Targeting the podocyte cytoskeleton: from pathogenesis to therapy in proteinuric kidney disease*. Nephrol Dial Transplant, 2016. **31**(10): p. 1577-83.
8. Kerjaschki, D., *Caught flat-footed: podocyte damage and the molecular bases of focal glomerulosclerosis*. J Clin Invest, 2001. **108**(11): p. 1583-7.
9. Chiang, C.K. and R. Inagi, *Glomerular diseases: genetic causes and future therapeutics*. Nat Rev Nephrol, 2010. **6**(9): p. 539-54.
10. Guruswamy Sangameswaran, K.D. and K.M. Baradhi, *Focal Segmental Glomerulosclerosis*, in *StatPearls*. 2022: Treasure Island (FL).
11. Rosenberg, A.Z. and J.B. Kopp, *Focal Segmental Glomerulosclerosis*. Clin J Am Soc Nephrol, 2017. **12**(3): p. 502-517.
12. Kriz, W. and K.V. Lemley, *Mechanical challenges to the glomerular filtration barrier: adaptations and pathway to sclerosis*. Pediatr Nephrol, 2017. **32**(3): p. 405-417.
13. Fukasawa, H., S. Bornheimer, K. Kudlicka, and M.G. Farquhar, *Slit diaphragms contain tight junction proteins*. J Am Soc Nephrol, 2009. **20**(7): p. 1491-503.
14. Ruotsalainen, V., P. Ljungberg, J. Wartiovaara, U. Lenkkeri, M. Kestila, H. Jalanko, C. Holmberg, and K. Tryggvason, *Nephrin is specifically located at the slit diaphragm of glomerular podocytes*. Proc Natl Acad Sci U S A, 1999. **96**(14): p. 7962-7.
15. Verma, R., M. Venkatarreddy, A. Kalinowski, S.R. Patel, and P. Garg, *Integrin Ligation Results in Nephrin Tyrosine Phosphorylation In Vitro*. PLoS One, 2016. **11**(2): p. e0148906.
16. Verma, R., M. Venkatarreddy, A. Kalinowski, T. Li, J. Kukla, A. Mollin, G. Cara-Fuentes, S.R. Patel, and P. Garg, *Nephrin is necessary for podocyte recovery following injury in an adult mature glomerulus*. PLoS One, 2018. **13**(6): p. e0198013.
17. Putaala, H., R. Soinenen, P. Kilpelainen, J. Wartiovaara, and K. Tryggvason, *The murine nephrin gene is specifically expressed in kidney, brain and pancreas*:

- inactivation of the gene leads to massive proteinuria and neonatal death.* Hum Mol Genet, 2001. **10**(1): p. 1-8.
18. Takeuchi, K., S. Naito, N. Kawashima, N. Ishigaki, T. Sano, K. Kamata, and Y. Takeuchi, *New Anti-Nephrin Antibody Mediated Podocyte Injury Model Using a C57BL/6 Mouse Strain.* Nephron, 2018. **138**(1): p. 71-87.
 19. Topham, P.S., H. Kawachi, S.A. Haydar, S. Chugh, T.A. Addona, K.B. Charron, L.B. Holzman, M. Shia, F. Shimizu, and D.J. Salant, *Nephritogenic mAb 5-1-6 is directed at the extracellular domain of rat nephrin.* J Clin Invest, 1999. **104**(11): p. 1559-66.
 20. Blaine, J. and J. Dylewski, *Regulation of the Actin Cytoskeleton in Podocytes.* Cells, 2020. **9**(7).
 21. Srivastava, T., H. Dai, D.P. Heruth, U.S. Alon, R.E. Garola, J. Zhou, R.S. Duncan, A. El-Meanawy, E.T. McCarthy, R. Sharma, M.L. Johnson, V.J. Savin, and M. Sharma, *Mechanotransduction signaling in podocytes from fluid flow shear stress.* Am J Physiol Renal Physiol, 2018. **314**(1): p. F22-F34.
 22. Kriz, W., I. Shirato, M. Nagata, M. LeHir, and K.V. Lemley, *The podocyte's response to stress: the enigma of foot process effacement.* Am J Physiol Renal Physiol, 2013. **304**(4): p. F333-47.
 23. Torban, E., F. Braun, N. Wanner, T. Takano, P.R. Goodyer, R. Lennon, P. Ronco, A.V. Cybulsky, and T.B. Huber, *From podocyte biology to novel cures for glomerular disease.* Kidney Int, 2019. **96**(4): p. 850-861.
 24. Zhang, Y., Y. Yoshida, M. Nameta, B. Xu, I. Taguchi, T. Ikeda, H. Fujinaka, S. Magdeldin, H. Tsukaguchi, Y. Harita, E. Yaoita, and T. Yamamoto, *Glomerular proteins related to slit diaphragm and matrix adhesion in the foot processes are highly tyrosine phosphorylated in the normal rat kidney.* Nephrol Dial Transplant, 2010. **25**(6): p. 1785-95.
 25. Nagata, M., *Podocyte injury and its consequences.* Kidney Int, 2016. **89**(6): p. 1221-30.
 26. Kriz, W. and K.V. Lemley, *A potential role for mechanical forces in the detachment of podocytes and the progression of CKD.* J Am Soc Nephrol, 2015. **26**(2): p. 258-69.
 27. Mundel, P. and S.J. Shankland, *Podocyte biology and response to injury.* J Am Soc Nephrol, 2002. **13**(12): p. 3005-15.
 28. Blanchoin, L., R. Boujemaa-Paterski, C. Sykes, and J. Plastino, *Actin dynamics, architecture, and mechanics in cell motility.* Physiol Rev, 2014. **94**(1): p. 235-63.
 29. Suleiman, H.Y., R. Roth, S. Jain, J.E. Heuser, A.S. Shaw, and J.H. Miner, *Injury-induced actin cytoskeleton reorganization in podocytes revealed by super-resolution microscopy.* JCI Insight, 2017. **2**(16).
 30. Deakin, N.O. and C.E. Turner, *Paxillin comes of age.* J Cell Sci, 2008. **121**(Pt 15): p. 2435-44.
 31. Legerstee, K., B. Geverts, J.A. Slotman, and A.B. Houtsmuller, *Dynamics and distribution of paxillin, vinculin, zyxin and VASP depend on focal adhesion location and orientation.* Sci Rep, 2019. **9**(1): p. 10460.
 32. Oakes, P.W. and M.L. Gardel, *Stressing the limits of focal adhesion mechanosensitivity.* Curr Opin Cell Biol, 2014. **30**: p. 68-73.
 33. Fan, L., S. Pellegrin, A. Scott, and H. Mellor, *The small GTPase Rif is an alternative trigger for the formation of actin stress fibers in epithelial cells.* J Cell Sci, 2010. **123**(Pt 8): p. 1247-52.

34. Couchman, J.R. and D.A. Rees, *Actomyosin organisation for adhesion, spreading, growth and movement in chick fibroblasts*. Cell Biol Int Rep, 1979. **3**(5): p. 431-9.
35. Rajah, A., C.G. Boudreau, A. Ilie, T.L. Wee, K. Tang, A.Z. Borisov, J. Orlowski, and C.M. Brown, *Paxillin S273 Phosphorylation Regulates Adhesion Dynamics and Cell Migration through a Common Protein Complex with PAK1 and betaPIX*. Sci Rep, 2019. **9**(1): p. 11430.
36. Nayal, A., D.J. Webb, C.M. Brown, E.M. Schaefer, M. Vicente-Manzanares, and A.R. Horwitz, *Paxillin phosphorylation at Ser273 localizes a GIT1-PIX-PAK complex and regulates adhesion and protrusion dynamics*. J Cell Biol, 2006. **173**(4): p. 587-9.
37. Wehrle-Haller, B., *Structure and function of focal adhesions*. Curr Opin Cell Biol, 2012. **24**(1): p. 116-24.
38. Ha, T.S., *Roles of adaptor proteins in podocyte biology*. World J Nephrol, 2013. **2**(1): p. 1-10.
39. Sachs, N. and A. Sonnenberg, *Cell-matrix adhesion of podocytes in physiology and disease*. Nat Rev Nephrol, 2013. **9**(4): p. 200-10.
40. Pozzi, A., G. Jarad, G.W. Moeckel, S. Coffa, X. Zhang, L. Gewin, V. Eremina, B.G. Hudson, D.B. Borza, R.C. Harris, L.B. Holzman, C.L. Phillips, R. Fassler, S.E. Quaggin, J.H. Miner, and R. Zent, *Beta1 integrin expression by podocytes is required to maintain glomerular structural integrity*. Dev Biol, 2008. **316**(2): p. 288-301.
41. Kreidberg, J.A., M.J. Donovan, S.L. Goldstein, H. Rennke, K. Shepherd, R.C. Jones, and R. Jaenisch, *Alpha 3 beta 1 integrin has a crucial role in kidney and lung organogenesis*. Development, 1996. **122**(11): p. 3537-47.
42. Has, C., G. Sparta, D. Kiritsi, L. Weibel, A. Moeller, V. Vega-Warner, A. Waters, Y. He, Y. Anikster, P. Esser, B.K. Straub, I. Hausser, D. Bockenbauer, B. Dekel, F. Hildebrandt, L. Bruckner-Tuderman, and G.F. Laube, *Integrin alpha3 mutations with kidney, lung, and skin disease*. N Engl J Med, 2012. **366**(16): p. 1508-14.
43. Greka, A. and P. Mundel, *Cell biology and pathology of podocytes*. Annu Rev Physiol, 2012. **74**: p. 299-323.
44. Al-Zahrani, K.N., K.D. Baron, and L.A. Sabourin, *Ste20-like kinase SLK, at the crossroads: a matter of life and death*. Cell Adh Migr, 2013. **7**(1): p. 1-10.
45. Wu, C., V.M. Keivens, T.E. O'Toole, J.A. McDonald, and M.H. Ginsberg, *Integrin activation and cytoskeletal interaction are essential for the assembly of a fibronectin matrix*. Cell, 1995. **83**(5): p. 715-24.
46. Webb, D.J., K. Donais, L.A. Whitmore, S.M. Thomas, C.E. Turner, J.T. Parsons, and A.F. Horwitz, *FAK-Src signalling through paxillin, ERK and MLCK regulates adhesion disassembly*. Nat Cell Biol, 2004. **6**(2): p. 154-61.
47. Legerstee, K. and A.B. Houtsmuller, *A Layered View on Focal Adhesions*. Biology (Basel), 2021. **10**(11).
48. Kuo, J.C., X. Han, J.R. Yates, 3rd, and C.M. Waterman, *Isolation of focal adhesion proteins for biochemical and proteomic analysis*. Methods Mol Biol, 2012. **757**: p. 297-323.
49. Wu, C., *Focal adhesion: a focal point in current cell biology and molecular medicine*. Cell Adh Migr, 2007. **1**(1): p. 13-8.
50. Lopez-Colome, A.M., I. Lee-Rivera, R. Benavides-Hidalgo, and E. Lopez, *Paxillin: a crossroad in pathological cell migration*. J Hematol Oncol, 2017. **10**(1): p. 50.
51. Ripamonti, M., N. Liaudet, L. Azizi, D. Bouvard, V.P. Hytonen, and B. Wehrle-Haller, *Structural and functional analysis of LIM domain-dependent recruitment of*

- paxillin to alphavbeta3 integrin-positive focal adhesions*. *Commun Biol*, 2021. **4**(1): p. 380.
52. Zamir, E. and B. Geiger, *Molecular complexity and dynamics of cell-matrix adhesions*. *J Cell Sci*, 2001. **114**(Pt 20): p. 3583-90.
 53. Lausecker, F., X. Tian, K. Inoue, Z. Wang, C.E. Pedigo, H. Hassan, C. Liu, M. Zimmer, S. Jinno, A.L. Huckle, H. Hamidi, R.S. Ross, R. Zent, C. Ballestrem, R. Lennon, and S. Ishibe, *Vinculin is required to maintain glomerular barrier integrity*. *Kidney Int*, 2018. **93**(3): p. 643-655.
 54. Shahbazi, R., B. Baradaran, M. Khordadmehr, S. Safaei, A. Baghbanzadeh, F. Jigari, and H. Ezzati, *Targeting ROCK signaling in health, malignant and non-malignant diseases*. *Immunol Lett*, 2020. **219**: p. 15-26.
 55. Humphries, J.D., P. Wang, C. Streuli, B. Geiger, M.J. Humphries, and C. Ballestrem, *Vinculin controls focal adhesion formation by direct interactions with talin and actin*. *J Cell Biol*, 2007. **179**(5): p. 1043-57.
 56. Subauste, M.C., O. Pertz, E.D. Adamson, C.E. Turner, S. Junger, and K.M. Hahn, *Vinculin modulation of paxillin-FAK interactions regulates ERK to control survival and motility*. *J Cell Biol*, 2004. **165**(3): p. 371-81.
 57. Turner, C.E., *Paxillin interactions*. *J Cell Sci*, 2000. **113 Pt 23**: p. 4139-40.
 58. Tian, X., J.J. Kim, S.M. Monkley, N. Gotoh, R. Nandez, K. Soda, K. Inoue, D.M. Balkin, H. Hassan, S.H. Son, Y. Lee, G. Moeckel, D.A. Calderwood, L.B. Holzman, D.R. Critchley, R. Zent, J. Reiser, and S. Ishibe, *Podocyte-associated talin1 is critical for glomerular filtration barrier maintenance*. *J Clin Invest*, 2014. **124**(3): p. 1098-113.
 59. Chinthalapudi, K., E.S. Rangarajan, and T. Izard, *The interaction of talin with the cell membrane is essential for integrin activation and focal adhesion formation*. *Proc Natl Acad Sci U S A*, 2018. **115**(41): p. 10339-10344.
 60. Elliott, P.R., B.T. Goult, P.M. Kopp, N. Bate, J.G. Grossmann, G.C. Roberts, D.R. Critchley, and I.L. Barsukov, *The Structure of the talin head reveals a novel extended conformation of the FERM domain*. *Structure*, 2010. **18**(10): p. 1289-99.
 61. Gingras, A.R., N. Bate, B.T. Goult, B. Patel, P.M. Kopp, J. Emsley, I.L. Barsukov, G.C. Roberts, and D.R. Critchley, *Central region of talin has a unique fold that binds vinculin and actin*. *J Biol Chem*, 2010. **285**(38): p. 29577-87.
 62. Zhang, X., G. Jiang, Y. Cai, S.J. Monkley, D.R. Critchley, and M.P. Sheetz, *Talin depletion reveals independence of initial cell spreading from integrin activation and traction*. *Nat Cell Biol*, 2008. **10**(9): p. 1062-8.
 63. Gingras, A.R., W.H. Ziegler, A.A. Bobkov, M.G. Joyce, D. Fasci, M. Himmel, S. Rothemund, A. Ritter, J.G. Grossmann, B. Patel, N. Bate, B.T. Goult, J. Emsley, I.L. Barsukov, G.C. Roberts, R.C. Liddington, M.H. Ginsberg, and D.R. Critchley, *Structural determinants of integrin binding to the talin rod*. *J Biol Chem*, 2009. **284**(13): p. 8866-76.
 64. Luhovy, A.Y., A. Jaber, J. Papillon, J. Guillemette, and A.V. Cybulsky, *Regulation of the Ste20-like kinase, SLK: involvement of activation segment phosphorylation*. *J Biol Chem*, 2012. **287**(8): p. 5446-58.
 65. Delarosa, S., J. Guillemette, J. Papillon, Y.S. Han, A.S. Kristof, and A.V. Cybulsky, *Activity of the Ste20-like kinase, SLK, is enhanced by homodimerization*. *Am J Physiol Renal Physiol*, 2011. **301**(3): p. F554-64.

66. Jaber, A., E. Hooker, J. Guillemette, J. Papillon, A.S. Kristof, and A.V. Cybulsky, *Identification of Tpr and alpha-actinin-4 as two novel SLK-interacting proteins*. *Biochim Biophys Acta*, 2015. **1853**(10 Pt A): p. 2539-52.
67. Cybulsky, A.V., J. Guillemette, J. Papillon, and N.T. Abouelazm, *Regulation of Ste20-like kinase, SLK, activity: Dimerization and activation segment phosphorylation*. *PLoS One*, 2017. **12**(5): p. e0177226.
68. Al-Zahrani, K.N., P. Sekhon, D.R. Tessier, J. Yockell-Lelievre, B.R. Pryce, K.D. Baron, G.A. Howe, R.K. Sriram, K. Daniel, M. McKay, V. Lo, J. Quizi, C.L. Addison, A. Gruslin, and L.A. Sabourin, *Essential role for the SLK protein kinase in embryogenesis and placental tissue development*. *Dev Dyn*, 2014. **243**(5): p. 640-51.
69. Sabourin, L.A., K. Tamai, P. Seale, J. Wagner, and M.A. Rudnicki, *Caspase 3 cleavage of the Ste20-related kinase SLK releases and activates an apoptosis-inducing kinase domain and an actin-disassembling region*. *Mol Cell Biol*, 2000. **20**(2): p. 684-96.
70. O'Reilly, P.G., S. Wagner, D.J. Franks, K. Cailliau, E. Browaeys, C. Dissous, and L.A. Sabourin, *The Ste20-like kinase SLK is required for cell cycle progression through G2*. *J Biol Chem*, 2005. **280**(51): p. 42383-90.
71. Guilluy, C., M. Rolli-Derkinderen, L. Loufrani, A. Bourge, D. Henrion, L. Sabourin, G. Loirand, and P. Pacaud, *Ste20-related kinase SLK phosphorylates Ser188 of RhoA to induce vasodilation in response to angiotensin II Type 2 receptor activation*. *Circ Res*, 2008. **102**(10): p. 1265-74.
72. Fokin, A.I., T.S. Klementeva, E.S. Nadezhkina, and A.V. Burakov, *SLK/LOS kinase regulates cell motility independently of microtubule organization and Golgi polarization*. *Cytoskeleton (Hoboken)*, 2016. **73**(2): p. 83-92.
73. Quizi, J.L., K. Baron, K.N. Al-Zahrani, P. O'Reilly, R.K. Sriram, J. Conway, A.A. Laurin, and L.A. Sabourin, *SLK-mediated phosphorylation of paxillin is required for focal adhesion turnover and cell migration*. *Oncogene*, 2013. **32**(39): p. 4656-63.
74. Cybulsky, A.V., J. Papillon, J. Guillemette, N. Belkina, G. Patino-Lopez, and E. Torban, *Ste20-like kinase, SLK, a novel mediator of podocyte integrity*. *Am J Physiol Renal Physiol*, 2018. **315**(1): p. F186-F198.
75. Hao, W., T. Takano, J. Guillemette, J. Papillon, G. Ren, and A.V. Cybulsky, *Induction of apoptosis by the Ste20-like kinase SLK, a germinal center kinase that activates apoptosis signal-regulating kinase and p38*. *J Biol Chem*, 2006. **281**(6): p. 3075-84.
76. Cybulsky, A.V., T. Takano, J. Papillon, J. Guillemette, A.M. Herzenberg, and C.R. Kennedy, *Podocyte injury and albuminuria in mice with podocyte-specific overexpression of the Ste20-like kinase, SLK*. *Am J Pathol*, 2010. **177**(5): p. 2290-9.
77. Marshall, C.B., R.D. Krofft, J.W. Pippin, and S.J. Shankland, *CDK inhibitor p21 is prosurvival in adriamycin-induced podocyte injury, in vitro and in vivo*. *Am J Physiol Renal Physiol*, 2010. **298**(5): p. F1140-51.
78. Lee, V.W. and D.C. Harris, *Adriamycin nephropathy: a model of focal segmental glomerulosclerosis*. *Nephrology (Carlton)*, 2011. **16**(1): p. 30-8.
79. Papeta, N., Z. Zheng, E.A. Schon, S. Brosel, M.M. Altintas, S.H. Nasr, J. Reiser, V.D. D'Agati, and A.G. Gharavi, *Prkdc participates in mitochondrial genome maintenance and prevents Adriamycin-induced nephropathy in mice*. *J Clin Invest*, 2010. **120**(11): p. 4055-64.

80. Wang, Y., Y.P. Wang, Y.C. Tay, and D.C. Harris, *Progressive adriamycin nephropathy in mice: sequence of histologic and immunohistochemical events*. *Kidney Int*, 2000. **58**(4): p. 1797-804.
81. Woychyshyn, B., J. Papillon, J. Guillemette, J.R. Navarro-Betancourt, and A.V. Cybulsky, *Genetic ablation of SLK exacerbates glomerular injury in adriamycin nephrosis in mice*. *Am J Physiol Renal Physiol*, 2020. **318**(6): p. F1377-F1390.
82. Viswanatha, R., P.Y. Ohouo, M.B. Smolka, and A. Bretscher, *Local phosphocycling mediated by LOK/SLK restricts ezrin function to the apical aspect of epithelial cells*. *J Cell Biol*, 2012. **199**(6): p. 969-84.
83. Bachir, A.I., A.R. Horwitz, W.J. Nelson, and J.M. Bianchini, *Actin-Based Adhesion Modules Mediate Cell Interactions with the Extracellular Matrix and Neighboring Cells*. *Cold Spring Harb Perspect Biol*, 2017. **9**(7).
84. Takeda, T., *Podocyte cytoskeleton is connected to the integral membrane protein podocalyxin through Na⁺/H⁺-exchanger regulatory factor 2 and ezrin*. *Clin Exp Nephrol*, 2003. **7**(4): p. 260-9.
85. Katzemich, A., J.Y. Long, V. Panneton, L.A.B. Fisher, D. Hipfner, and F. Schock, *Slik phosphorylation of Talin T152 is crucial for proper Talin recruitment and maintenance of muscle attachment in Drosophila*. *Development*, 2019. **146**(20).
86. Horzum, U., B. Ozdil, and D. Pesen-Okvur, *Step-by-step quantitative analysis of focal adhesions*. *MethodsX*, 2014. **1**: p. 56-9.
87. Kachurina, N., C.F. Chung, E. Benderoff, S. Babayeva, M. Bitzan, P. Goodyer, T. Kitzler, D. Matar, A.V. Cybulsky, N. Alachkar, and E. Torban, *Novel unbiased assay for circulating podocyte-toxic factors associated with recurrent focal segmental glomerulosclerosis*. *Am J Physiol Renal Physiol*, 2016. **310**(10): p. F1148-56.
88. Bao, H., Y. Ge, A. Peng, and R. Gong, *Fine-tuning of NFkappaB by glycogen synthase kinase 3beta directs the fate of glomerular podocytes upon injury*. *Kidney Int*, 2015. **87**(6): p. 1176-90.
89. Dunn, K.W., M.M. Kamocka, and J.H. McDonald, *A practical guide to evaluating colocalization in biological microscopy*. *Am J Physiol Cell Physiol*, 2011. **300**(4): p. C723-42.
90. Tadokoro, S., S.J. Shattil, K. Eto, V. Tai, R.C. Liddington, J.M. de Pereda, M.H. Ginsberg, and D.A. Calderwood, *Talin binding to integrin beta tails: a final common step in integrin activation*. *Science*, 2003. **302**(5642): p. 103-6.
91. Dlugos, C.P., C. Picciotto, C. Lepa, M. Krakow, A. Stober, M.L. Eddy, T. Weide, A. Jeibmann, P.K. M, V. Van Marck, J. Klingauf, A. Ricker, R. Wedlich-Soldner, H. Pavenstadt, C. Klambt, and B. George, *Nephrin Signaling Results in Integrin beta1 Activation*. *J Am Soc Nephrol*, 2019. **30**(6): p. 1006-1019.
92. Lock, F.E., K.R. Ryan, N.S. Poulter, M. Parsons, and N.A. Hotchin, *Differential regulation of adhesion complex turnover by ROCK1 and ROCK2*. *PLoS One*, 2012. **7**(2): p. e31423.
93. Brown, M.C., J.A. Perrotta, and C.E. Turner, *Identification of LIM3 as the principal determinant of paxillin focal adhesion localization and characterization of a novel motif on paxillin directing vinculin and focal adhesion kinase binding*. *J Cell Biol*, 1996. **135**(4): p. 1109-23.
94. Zaidel-Bar, R., R. Milo, Z. Kam, and B. Geiger, *A paxillin tyrosine phosphorylation switch regulates the assembly and form of cell-matrix adhesions*. *J Cell Sci*, 2007. **120**(Pt 1): p. 137-48.

95. Pasapera, A.M., I.C. Schneider, E. Rericha, D.D. Schlaepfer, and C.M. Waterman, *Myosin II activity regulates vinculin recruitment to focal adhesions through FAK-mediated paxillin phosphorylation*. *J Cell Biol*, 2010. **188**(6): p. 877-90.
96. Pryce, B.R., K.N. Al-Zahrani, S. Dufresne, N. Belkina, C. Labreche, G. Patino-Lopez, J. Frenette, S. Shaw, and L.A. Sabourin, *Deletion of the Ste20-like kinase SLK in skeletal muscle results in a progressive myopathy and muscle weakness*. *Skeletal Muscle*, 2017. **7**(1): p. 3.
97. Maywald, M.L., C. Picciotto, C. Lepa, L. Bertgen, F.S. Yousaf, A. Ricker, J. Klingauf, M.P. Krahn, H. Pavenstadt, and B. George, *Rap1 Activity Is Essential for Focal Adhesion and Slit Diaphragm Integrity*. *Front Cell Dev Biol*, 2022. **10**: p. 790365.
98. Kanasaki, K., Y. Kanda, K. Palmsten, H. Tanjore, S.B. Lee, V.S. Lebleu, V.H. Gattone, Jr., and R. Kalluri, *Integrin beta1-mediated matrix assembly and signaling are critical for the normal development and function of the kidney glomerulus*. *Dev Biol*, 2008. **313**(2): p. 584-93.
99. Celik, Y. and F. Celik, *Reduced podocyte expression of alpha3beta1 integrins and podocyte depletion in patients with primary focal segmental glomerulosclerosis and chronic PAN-treated rats*. *Transl Res*, 2006. **148**(1): p. 46.
100. Naylor, R.W., M. Morais, and R. Lennon, *Complexities of the glomerular basement membrane*. *Nat Rev Nephrol*, 2021. **17**(2): p. 112-127.
101. Timpl, R., H. Wiedemann, V. van Delden, H. Furthmayr, and K. Kuhn, *A network model for the organization of type IV collagen molecules in basement membranes*. *Eur J Biochem*, 1981. **120**(2): p. 203-11.